Introduction

The Nature of Seismic Reflection

Seismic reflections come from interfaces where the acoustic properties of the rocks change, and this fact is the basis of our understanding of the nature of seismic data. Acoustic impedance of a rock layer is the product of the density and the velocity of that layer, and strictly a reflection is generated by a contrast in acoustic impedance. In fact impedance and lithology normally follow each other, so that impedance boundaries and lithologic boundaries normally concur.

Consider a sand encased in shale, perhaps the most common situation forming a hydrocarbon reservoir. The shale-sand interface at the top generates a reflection, and the sand-shale interface at the base generates a reflection (Figure 1-1). Thus a sand has a reflection from the top and another from the base. These two reflections should be considered together in all studies of the reservoir sand.

At one location the sands normally have one impedance and the shales have another impedance. (Typically, sands have a lower impedance than shales in younger rocks and a higher impedance than shales in older rocks.) Thus the interfaces at top and base of a sand reservoir will almost always have impedance contrasts in the opposite sense. The sense of the impedance contrast determines the polarity of the seismic reflection, so that the top and base reflections for a sand reservoir encased in shale are opposite polarity from each other. This is a very significant piece of information used in the identification of reservoir reflections. Numerous figures in this book illustrate the pairing of top and base reflections — for example, Figure 1-20 and many figures in Chapters 2 and 5.

Tying of geologic data and seismic data together involves some knowledge of velocity, but the depth-to-time tie is not sufficient. We must identify seismic reflections on the basis of the character expected from the geologic interfaces and the fact that the layer of interest will normally have a top reflection and a base reflection. Consideration of the top and base reflections together involves the topics of natural pairing, choice of color schemes, data phase, data polarity, seismic resolution, and tuning, all of which are subjects of this book.

Philosophy of Seismic Interpretation

A proper understanding of seismic data is a necessary precursor to successful interpretation. Before horizon tracking commences the data must be qualified to understand what geologic information extraction is possible. The interpreter must consider data quality, frequency content, resolution, data phase, and data polarity, and must learn as much as possible about the data acquisition and processing (Appendix A). The interpreter must determine whether the data are fit-for-purpose, and not spend time conducting studies which have no chance of success. He must of course consider the background geology but should not be completely constrained by it. Modern 3-D

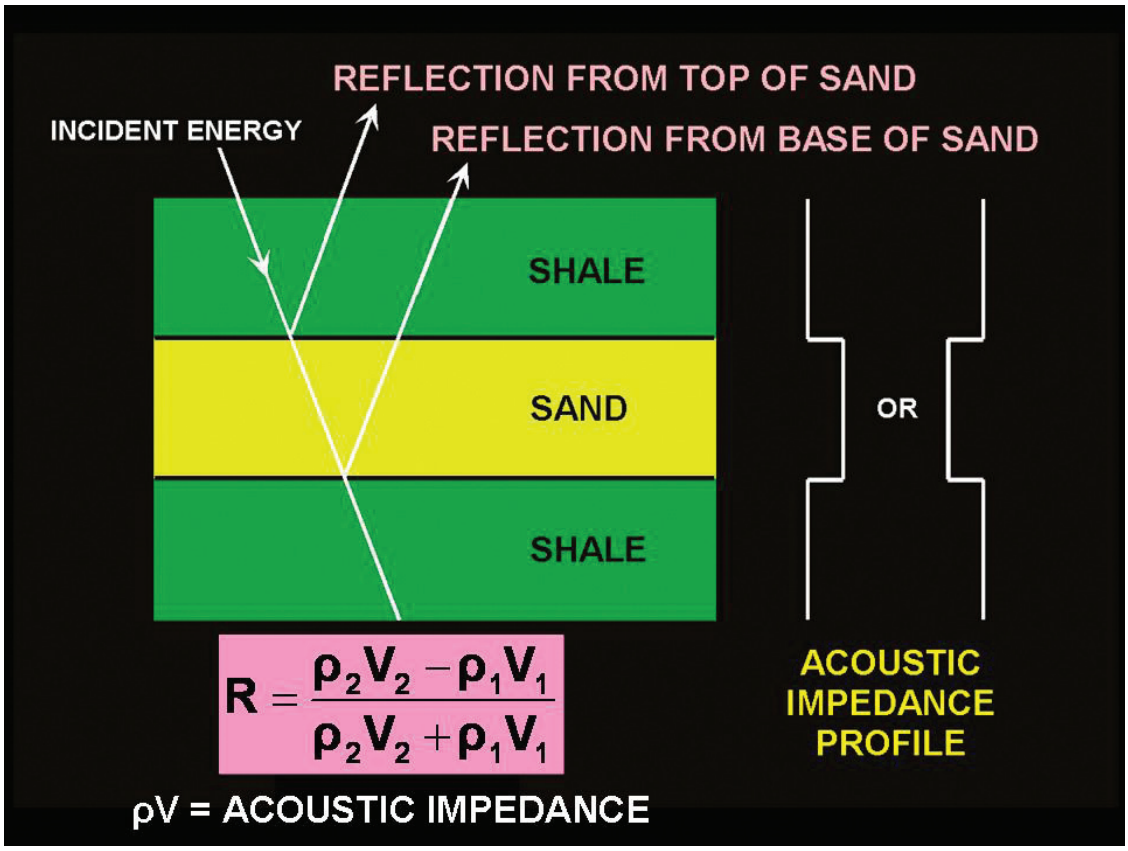

Fig. 1-1. Reflections come from interfaces, top and base of a sand reservoir.

seismic data can under some circumstances dictate a new geologic model.

Visualization is important today and always has been. Thinking in three dimensions is a critical ability of seismic interpreters. Three-dimensional seismic data match the dimensions of the data to the dimensions of the earth, and thus make visualization easier. But the greatest benefit of modern 3-D seismic data is their improved quality and resolution. There is typically an amazing amount of geologic detail in seismic data today, and the task of seismic interpretation is to extract it. Noise and spurious events are also present, so that the job of interpretation is to separate the desired geology from the unwanted noise. The better the data quality is understood, the better this separation can be accomplished.

Computer-driven workstations are the tools of seismic interpretation, and modern workstations contain an amazing array of capabilities. The challenge of the workstation user is thus to be aware of the possibilities and to select the tool appropriate to the objective. We do not use workstation capabilities only because they are fashionable. So the modern interpreter must integrate not only geology and geophysics but computer-intensive workstation technology as well. Technological synergism reigns but creative pragmatism retains its place.

History of 3-D Seismic Methods

The earth has always been three-dimensional, and the limitations of the old-fashioned 2-D seismic survey had long been recognized. The first 3-D seismic experiments were apparently conducted by Esso in the 1960s, and the first publication of their results was by Walton (1972). This early work lacked migration so the images were poor. Geophysical Service Inc. (GSI) was the first seismic service company to be involved, and they conducted a large-scale field experiment, with the support of six oil companies, in the state of New Mexico in 1972–74 (Schneider, 1998). Three-dimensional surveys were first performed on a contractual basis in 1975, and the following

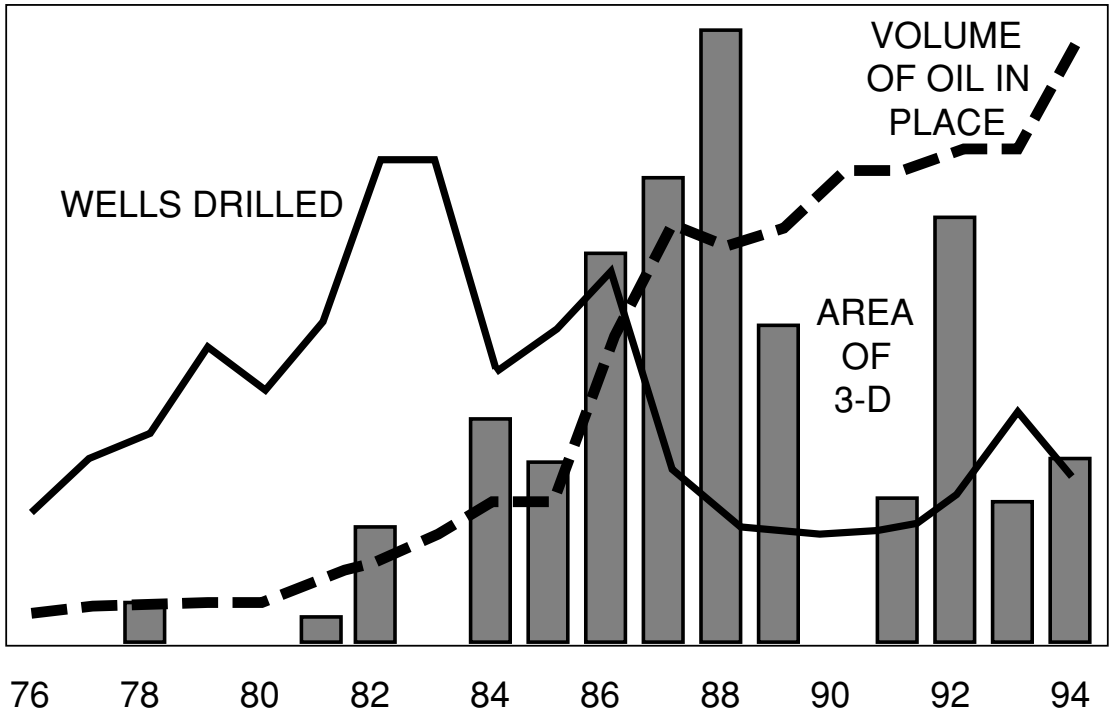

Fig. 1-2. Area covered by 3-D surveys, exploratory wells drilled and volume of oil in place for the period 1976 to 1994 in the Campos Basin offshore Brazil (from Martins et al., 1995). (Courtesy Petrobras.)

year Bone, Giles, and Tegland (1976) presented the technology to the world. The evolution and present state-of-the-art of the 3-D seismic method have been chronicled in a comprehensive reprint volume by Graebner, Hardage, and Schneider (2001).

The essence of the 3-D method is areal data collection followed by processing and interpretation of the closely spaced data volume. Initially 3-D was seen as expensive so its application was restricted to development applications (Tegland, 1977). In order to promote 3-D for exploration a widely spaced (and hence under-sampled) version was introduced, but this was not very successful. Today fully-sampled 3-D surveys are conducted on land, at sea, and in various transition zone environments.

The full economic benefit of 3-D seismic started to be appreciated in the late 1980s, as exemplified by this accolade:

> *"We acquired two offshore blocks which contained a total of seven competitor dry holes. Our exploration department drilled one more dry hole before making a discovery. At that point we conducted a 3-D survey while the platform was being prepared. When drilling commenced, guided by the 3-D data, we had 27 successful wells out of the next 28 drilled. In this erratic depositional environment, we believe such an accomplishment would not have been possible without the 3-D data."* (R. M. Wright, Chevron U.S.A. Inc, personal communication, 1988)

In the 1990s 3-D seismic surveys became mainstream, as Nestvold (1992) clearly demonstrates. Today mature petroleum areas are covered with 3-D data, often with many different vintages representing progressive improvements in technology. Martins et al. (1995), working in the Campos Basin offshore Brazil, have tracked the 3-D survey coverage in relation to the wells drilled and the oil reserves booked (Figure 1-2). This demonstrates very nicely that 3-D seismic can indeed replace the drilling of exploration wells. William Aylor, in the Foreword to this book, also demonstrates the business impact of 3-D seismic surveys.

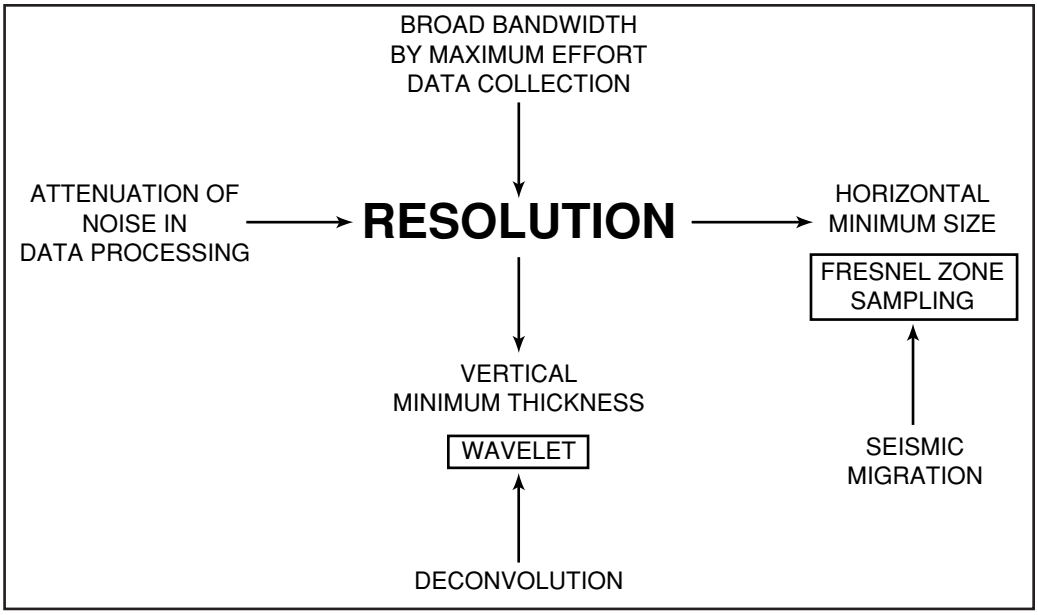

Fig. 1-3. Factors affecting horizontal and vertical seismic resolution.

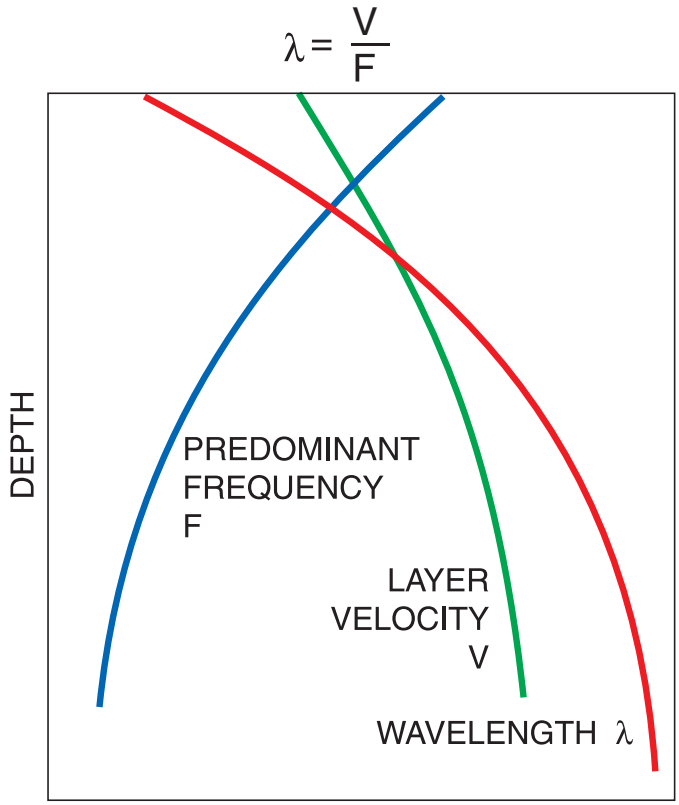

Fig. 1-4. Wavelength, the seismic measuring rod, increases significantly with depth making resolution poorer.

Resolution

The fundamental objective of a 3-D seismic survey is increased subsurface resolution. Resolution has both vertical and horizontal aspects and is significantly affected by the methods of data collection and processing (Figure 1-3). Sheriff (1985) discusses the subject qualitatively. The resolving power of seismic data is determined by the wavelength, which is defined as the distance in meters or feet from the crest of one reflection to the crest of the next one of the same color (polarity). The wavelength is calculated as the quotient of formation velocity and predominant frequency (Figure 1-4). Seismic velocity increases with depth because the rocks are older and more compacted. The predominant frequency decreases with depth because the higher frequencies in the seismic signal are more quickly attenuated. The result is that the size of the

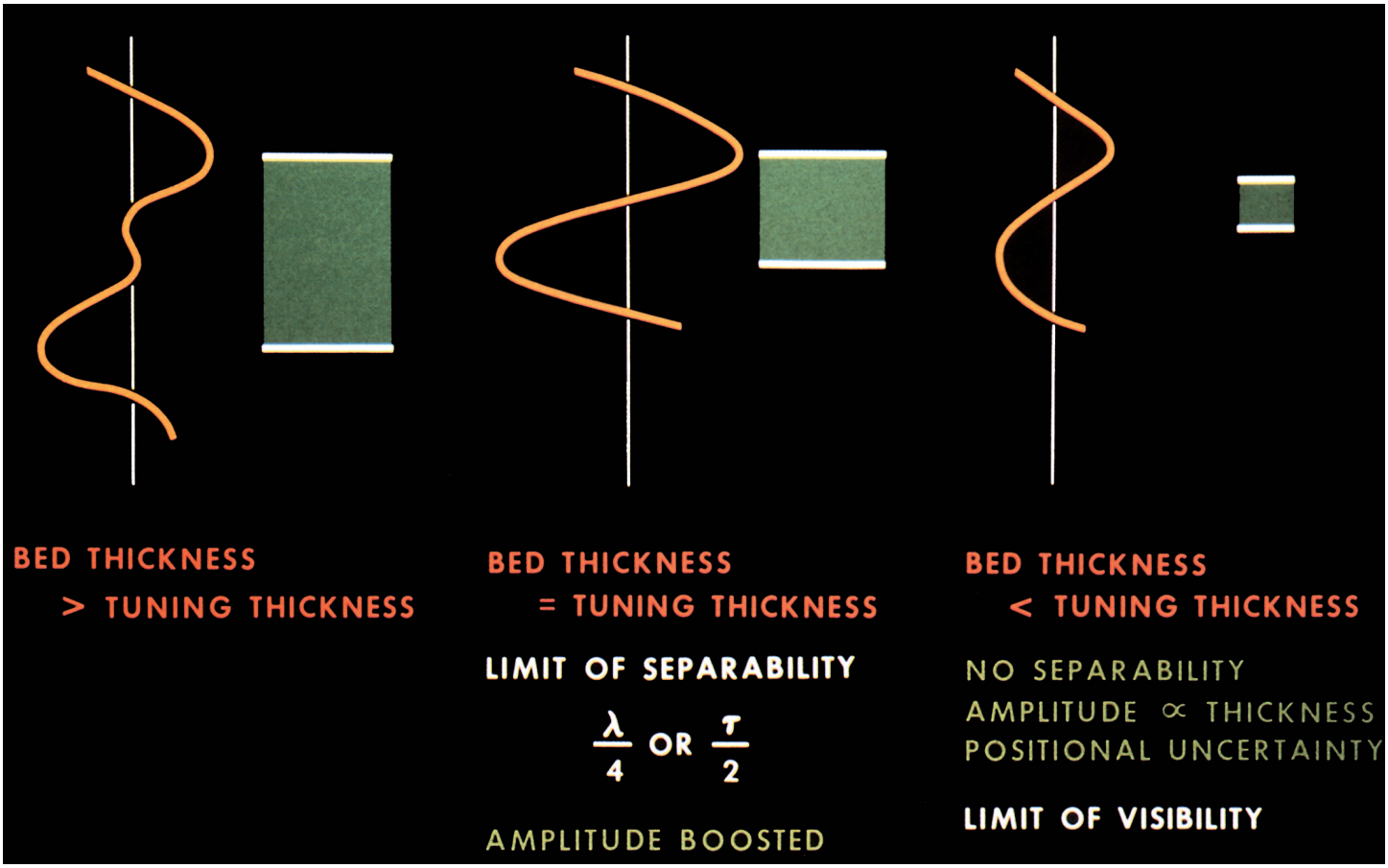

Fig. 1-5. Resolution of the reflections from the top and bottom of a bed is dependent on the interaction of closely spaced wavelets.

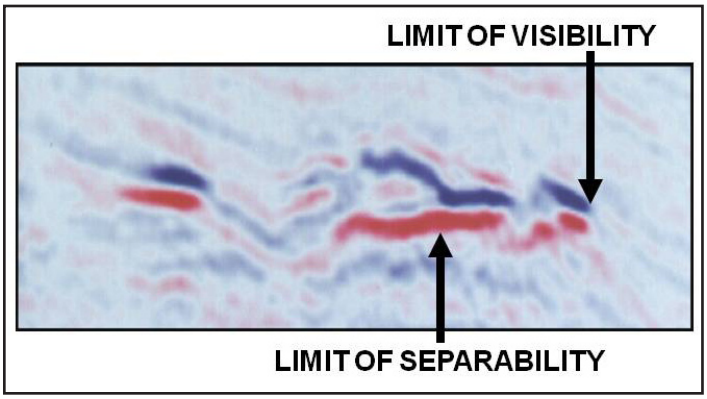

Fig. 1-6. Demonstration of Limit of separability and Limit of visibility.

wavelength increases significantly with depth, making resolution poorer.

Vertical resolution has two limits, both resulting from the interaction of the wavelets reflected from top and base of the bed under study. The **limit of separability** is equal to one-quarter of a wavelength (or half a period) and is simply the bed thickness corresponding to the closest separation of the two wavelets (Figure 1-5). For thinner beds than this, the top and base reflections are still visible but the amplitude is progressively attenuated until the **limit of visibility** is reached, when the reflected signal becomes obscured by the background noise. Figure 1-6 demonstrates clearly the concept of the two limits. The limit of visibility is a variable fraction of a wavelength and depends on the acoustic contrast of the layer of interest relative to the embedding material, the random and systematic noise in the data, and the phase of the seismic wavelet.

Table 1-1. Typical Limits of Visibility and Separability for a range of geologic situations.

			Age of rocks		VERY YOUNG	YOUNG	MEDIUM	OLD	VERY OLD
			Depth of target		VERY SHALLOW	SHALLOW	MEDIUM	DEEP	VERY DEEP
			Formation Velocity (m/s)		1600	2000	3500	5000	6000
			Predominant Frequency (Hz)		70	50	35	25	20
			Wavelength (m)	λ	23	40	100	200	300
			LIMIT OF SEPARABILITY	$\frac{\lambda}{4}$	**6**	**10**	**25**	**50**	**75**
LIMIT OF	VISIBILITY	Poor S/N	e.g. Water sand poor data	$\sim\frac{\lambda}{8}$	**3**	**5**	**13**	**25**	**38**
		Moderate S/N	e.g. Water or oil sand fairly good data	$\sim\frac{\lambda}{12}$	**2**	**3**	**8**	**17**	**25**
		High S/N	e.g. Gas sand good data	$\sim\frac{\lambda}{20}$	**1**	**2**	**5**	**10**	**15**
		Outstanding S/N	e.g. Gas sand excellent data	$\sim\frac{\lambda}{30}$	**<1**	**1**	**3**	**7**	**10**

units are meters

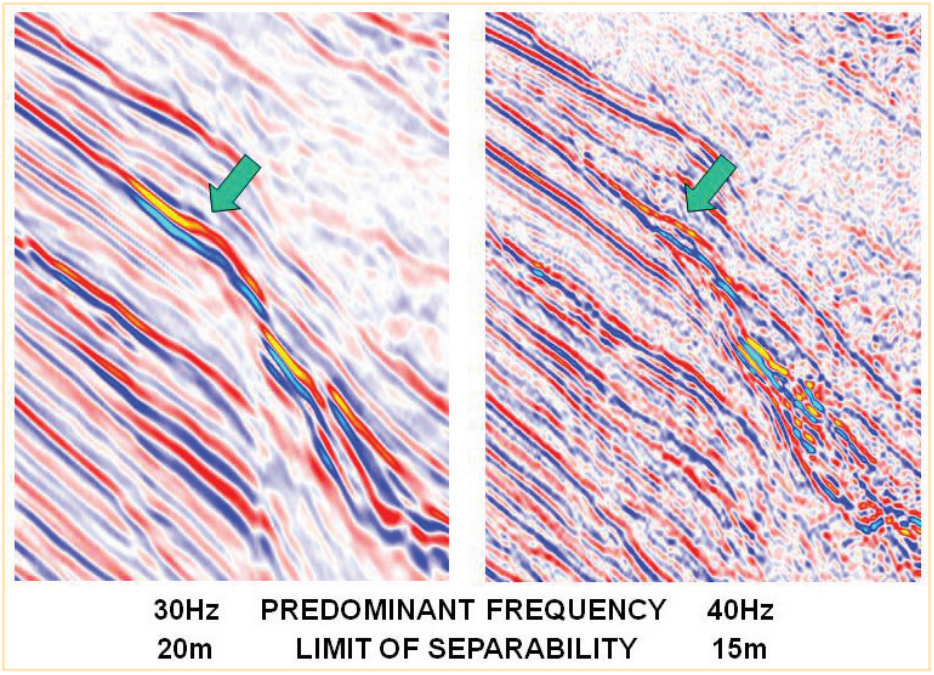

Fig. 1-7. The effect of frequency on the limit of separability. Note that top and base reflections (at green arrows) are well separated for the higher predominant frequency. (Courtesy Fugro GeoConsulting.)

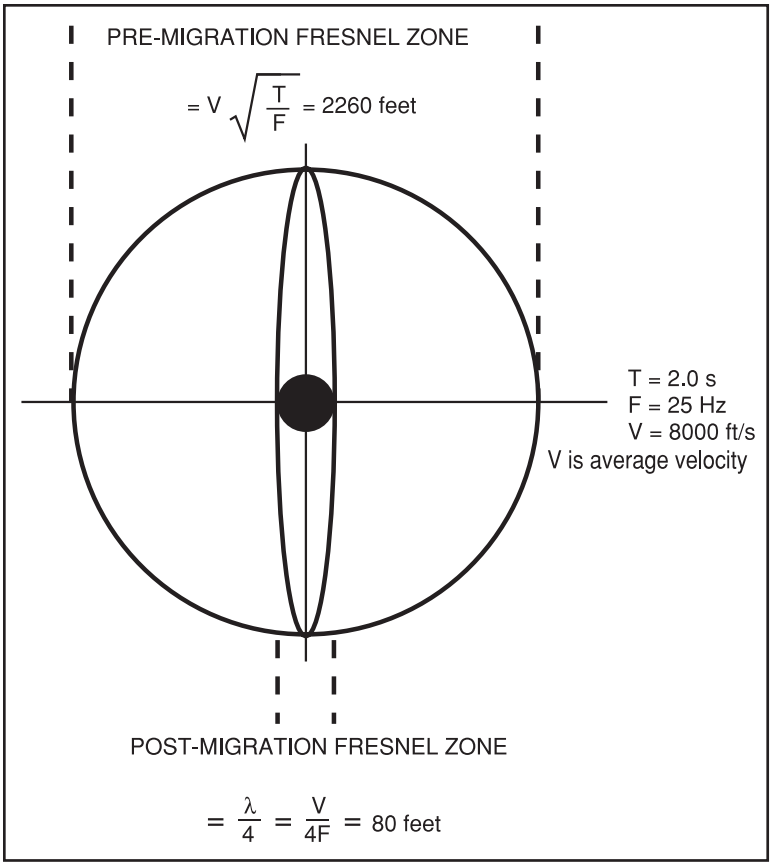

Fig. 1-8. Effect on Fresnel zone size and shape of 2-D and 3-D migration.

Table 1-2. Seismic visibility of a 5-meter sand.

Layer Velocity	Predominant Frequency	Wavelength	Sand 5 m
2000 m/s	40 Hz	50 m	λ/10
3000 m/s	30 Hz	100 m	λ/20
4000 m/s	20 Hz	200 m	λ/40

Table 1-1 illustrates five geologic situations of different rock ages and target depths. In order to calculate the resolution limits, one must think in terms of wavelength fractions and calculate the magnitude of the wavelength. The predominant frequency is determined by counting cycles in the data, and the layer velocity is estimated from a check-shot survey or a sonic log, or is guessed from knowledge of age, depth, and lithology. From predominant frequency and layer velocity, the wavelength and thus the limit of separability are directly calculated. Figure 1-7 shows two versions of the same data with very different predominant frequencies. Note the different amounts of separation between reflections, particularly at the position of the arrow.

For the limit of visibility, Table 1-1 offers four different wavelength fractions for different acoustic contrasts and signal-to-noise ratios. In this way the limit has been calculated for a matrix of twenty different situations, illustrating the enormous possible range in seismic visibility of thin beds. A rule-of-thumb based on the experience of the author is that the thinnest visible bed will be one-thirtieth of a wavelength, and this in the most favorable circumstances. If the reservoir of interest does not have a thickness above seismic visibility, then the study of reservoir porosity, net pay, lithology, etc. will not be possible. Table 1-2 converts 5 meters (postulated as the thickness of your reservoir) into wavelength fractions in three very different geologic situations. One-tenth of a wavelength should be visible in most circumstances, one-twentieth of a wavelength will be difficult to see seismically, and one-thirtieth probably will be invisible in all circumstances.

Migration is the principal technique for improving horizontal resolution, and in doing so it performs three distinct functions. The migration process (1) repositions reflections out-of-place because of dip, (2) focuses energy spread over a Fresnel zone, and (3) collapses diffraction patterns from points and edges. Seismic wavefronts travel in three dimensions and thus it is obvious that all the above are, in general, three-dimensional issues. If we treat them in two dimensions, we can only expect part of the

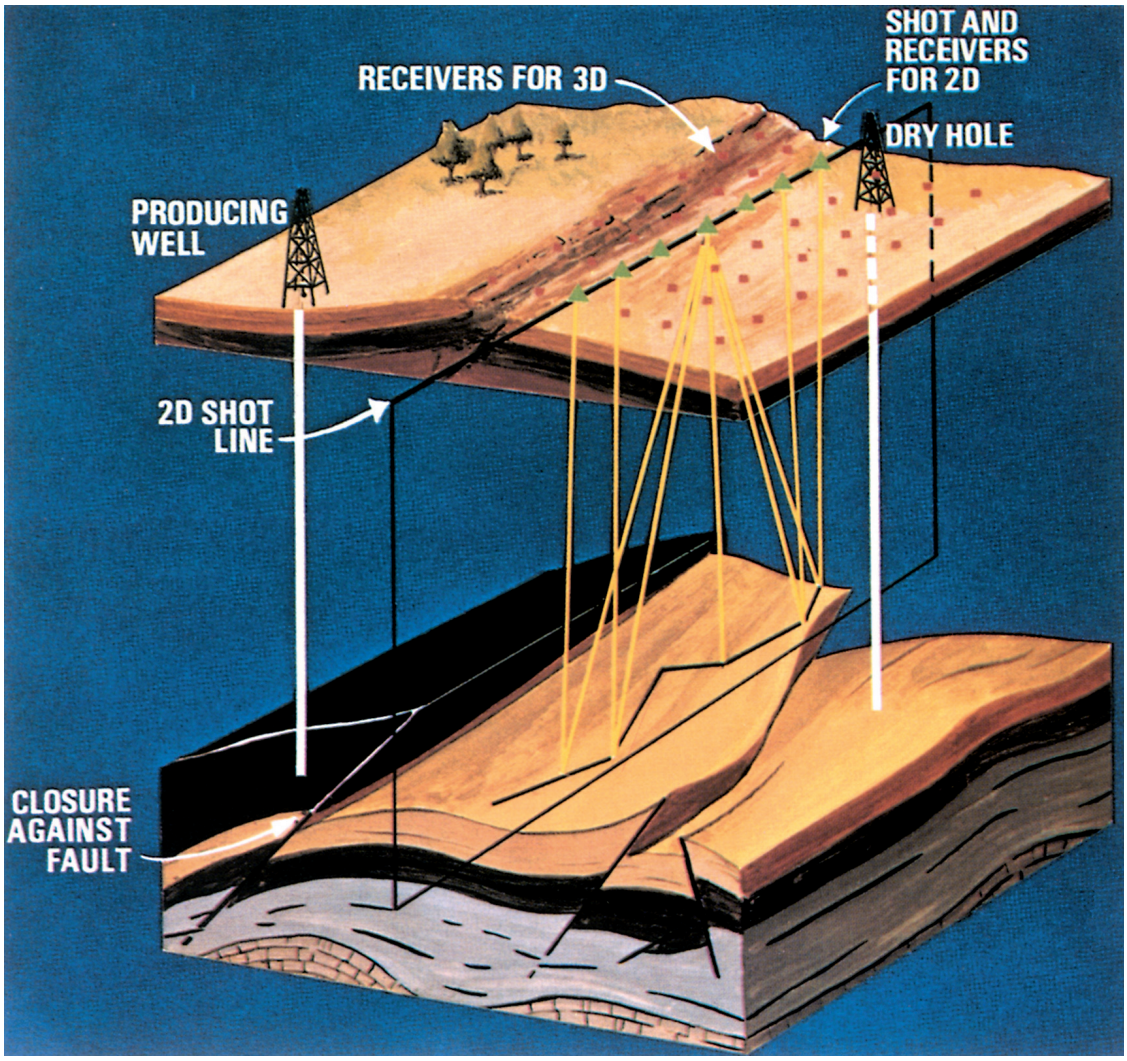

Fig. 1-9. Subsurface structure causes reflection points to lie outside the vertical plane through shots and receivers.

potential improvement. In practice, 2-D lines are often located with strike and dip of major features in mind so that the effect of the third dimension can be minimized, but never eliminated. Figure 1-8 shows the focusing effect of migration in two and three dimensions. The Fresnel zone will be reduced to an ellipse perpendicular to the line for 2-D migration (Lindsey, 1989) and to a small circle by 3-D migration. The diameter of one-quarter of a wavelength indicated in Figure 1-8 is for perfect migration. In practice, the residual Fresnel zone may be about twice this size.

The accuracy of 3-D migration depends on the velocity field, signal-to-noise ratio, migration aperture, and the approach used. Assuming the errors resulting from these factors are small, the data will be much more interpretable both structurally and stratigraphically. Intersecting events will be separated, the confusion of diffraction patterns will be gone, and dipping events will be moved to their correct subsurface positions. The collapsing of energy from diffractions and the focusing of energy spread over Fresnel zones will make amplitudes more accurate and more directly interpretable in terms of reservoir properties. In short the horizontal resolution of the data will be greatly improved.

Examples of 3-D Data Improvement

The interpreter of a 2-D vertical section normally assumes that the data were recorded in one vertical plane below the line traversed by the shots and receivers. The extent to which this is not so depends on the complexity of the structure perpendicular to the line. Figure 1-9 demonstrates that, in the presence of moderate structural

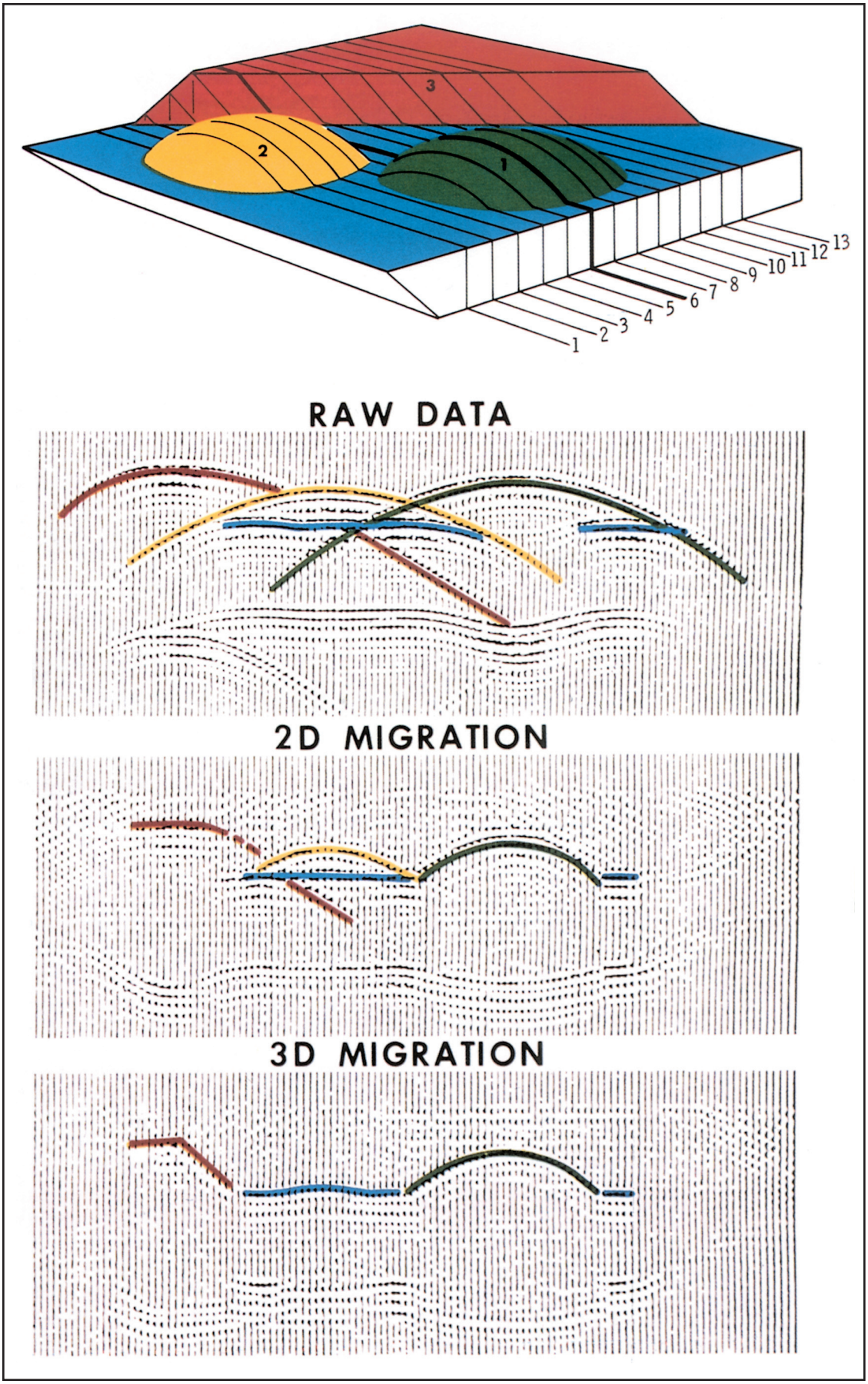

Fig. 1-10. Model of two anticlines and one fault with seismic data along Line 6 showing comparative effects of 2-D and 3-D migration (from French, 1974).

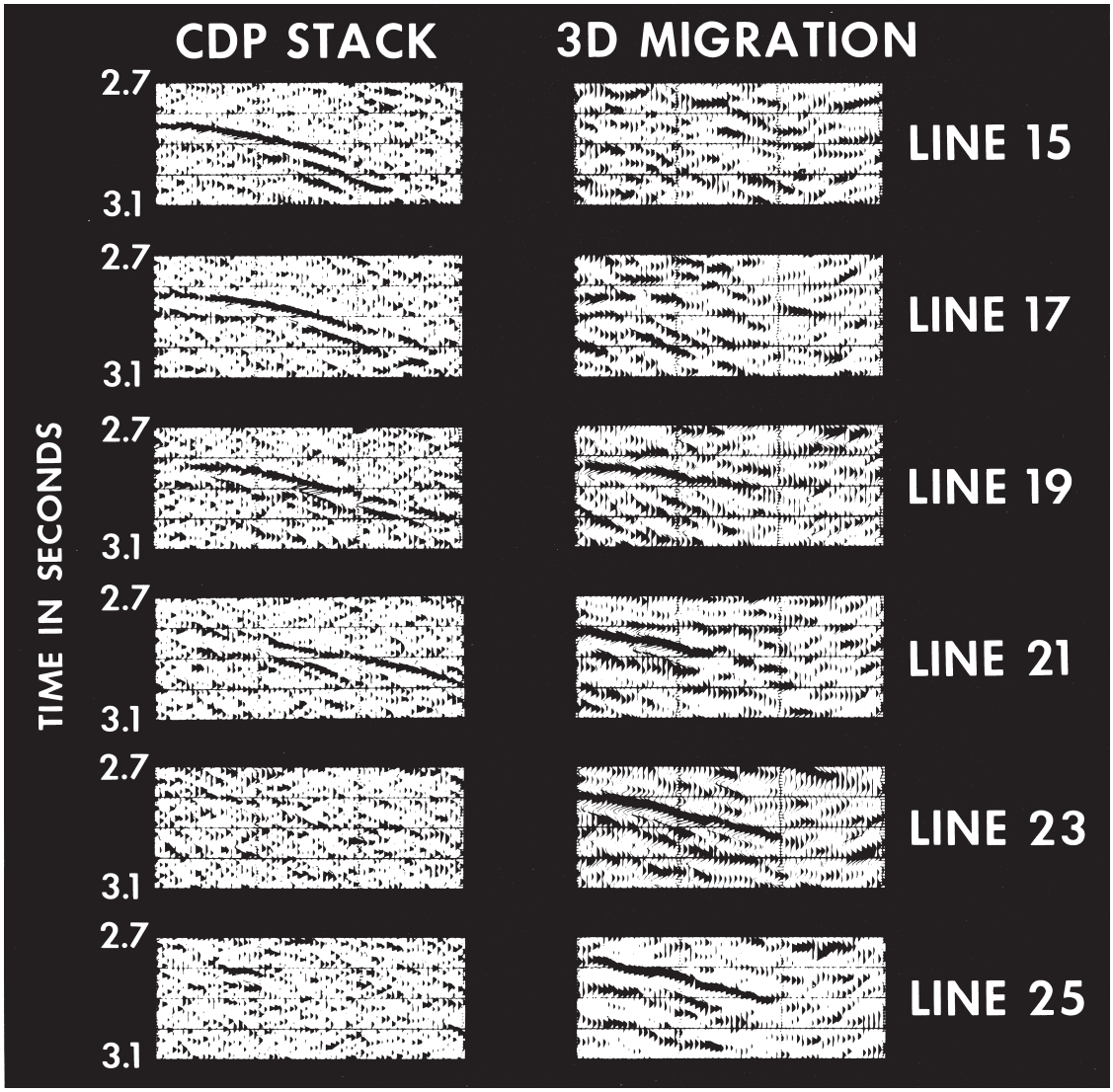

Fig. 1-11. Three-dimensional movement of a dipping reflection by 3-D migration. (Courtesy Geophysical Service Inc.)

complexity, the points at depth from which normal reflections are obtained may lie along an irregular zig-zag track. Only by migrating along *and* perpendicular to the line direction is it possible to resolve where these reflection points belong in the subsurface.

French (1974) demonstrated the value of 3-D migration very clearly in model experiments. He collected seismic data over a model containing two anticlines and a fault scarp (Figure 1-10). Thirteen lines of data were collected although only the results for Line 6 are shown. The raw data have diffraction patterns for both anticlines and the fault so the section appears very confused. The situation is greatly improved with 2-D migration and anticline number 1 (shown in green) is correctly imaged, as Line 6 passed over its crest. However, anticline number 2 (shown in yellow) should not occur on Line 6 and the fault scarp has the wrong slope. The 3-D migration has correctly imaged the fault scarp and moved the yellow anticline away from Line 6 to where it belongs.

Figure 1-11 demonstrates this three-dimensional event movement on real data. The same panel is presented before and after 3-D migration for six lines. Here we can observe the movement of a discrete patch of reflectivity to the left and in the direction of higher line numbers.

Figure 1-12 shows improved continuity of an unconformity reflection. The 2-D migration has collapsed most of the diffraction patterns but some confusion remains.

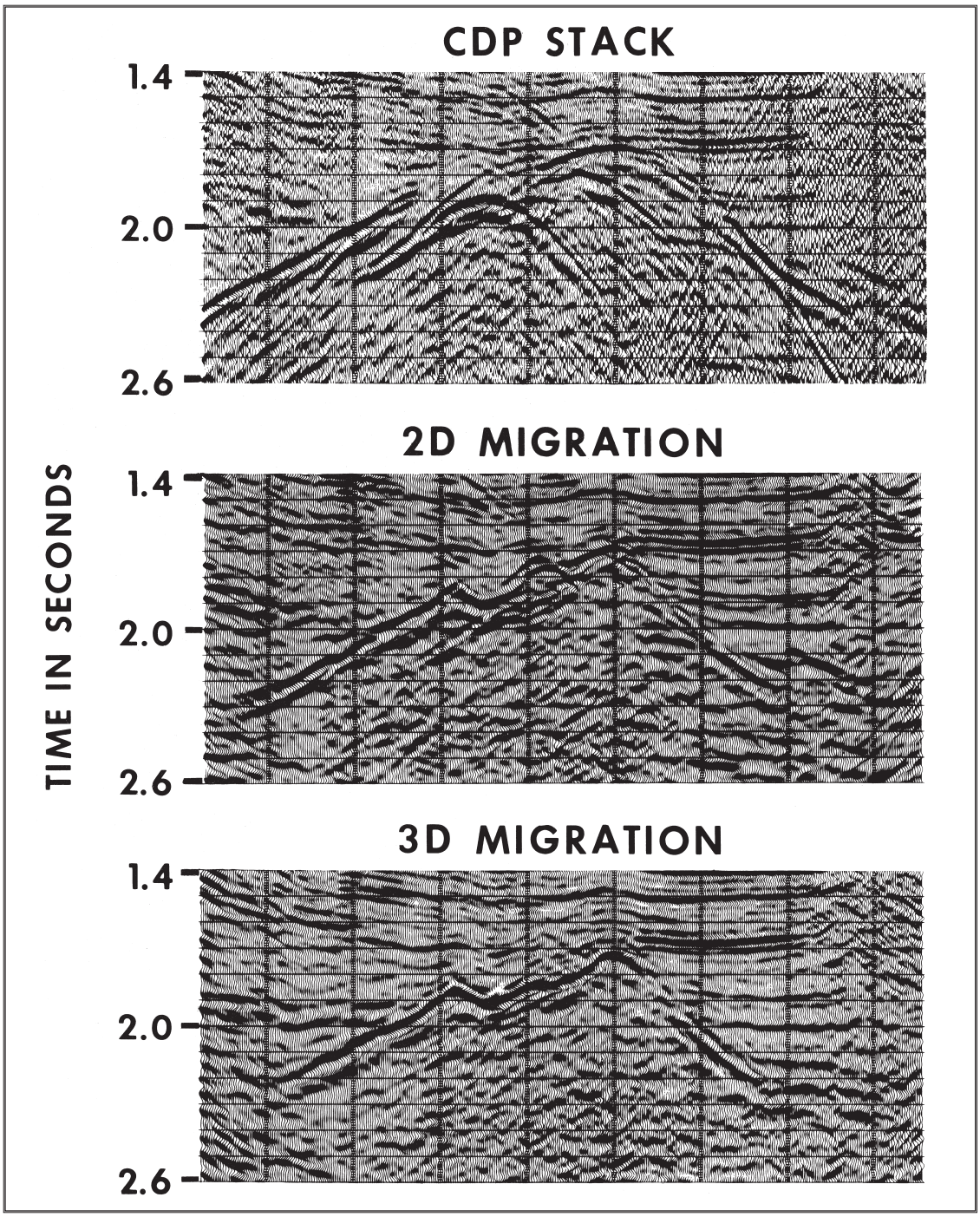

Fig. 1-12. Improved structural continuity of an unconformity reflection resulting from 2-D and 3-D migration.

The crossline component of the 3-D migration removes energy not in the plane of this section and clarifies the shape of the unconformity surface in significant detail.

Figure 1-13 shows the effect of 3-D migration in enhancing the visibility of a fluid contact reflection by removing energy not belonging in the plane of this section.

Figure 1-14 shows some major differences between the stacked and 3-D migrated versions of a line from Australia. It is easy to visualize the impact this change would have on an interpretation.

Figure 1-16 shows portions of three lines passing through and close to a salt diapir. Line 180 shows steeply dipping reflections at the edge of the salt mass, brought into place by the 3-D migration. Line 220 shows an apparent anticline which is caused by reflections dipping up steeply toward the salt face in a plane perpendicular to that of Figure 1-16. In this prospect, 3-D migration imaged reflections underneath a salt

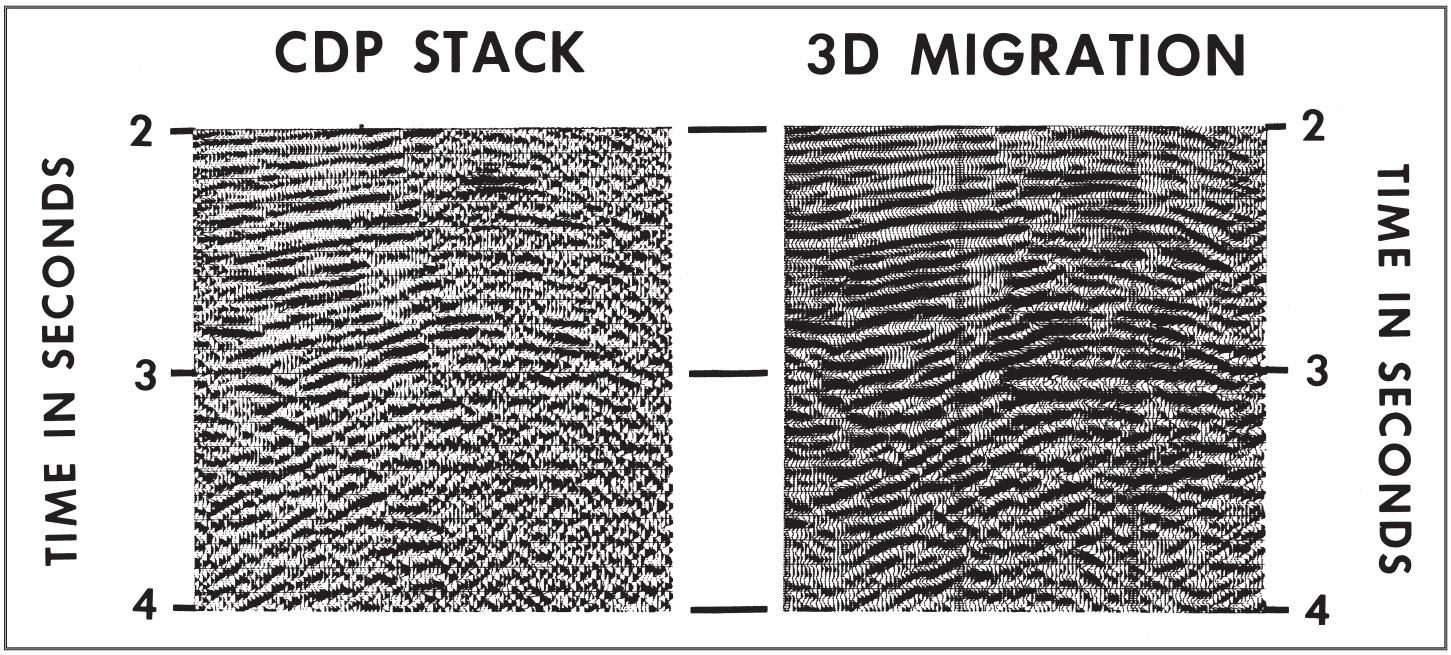

Fig. 1-13. Improved visibility of a flat spot reflection after removal of interfering events by 3-D migration.

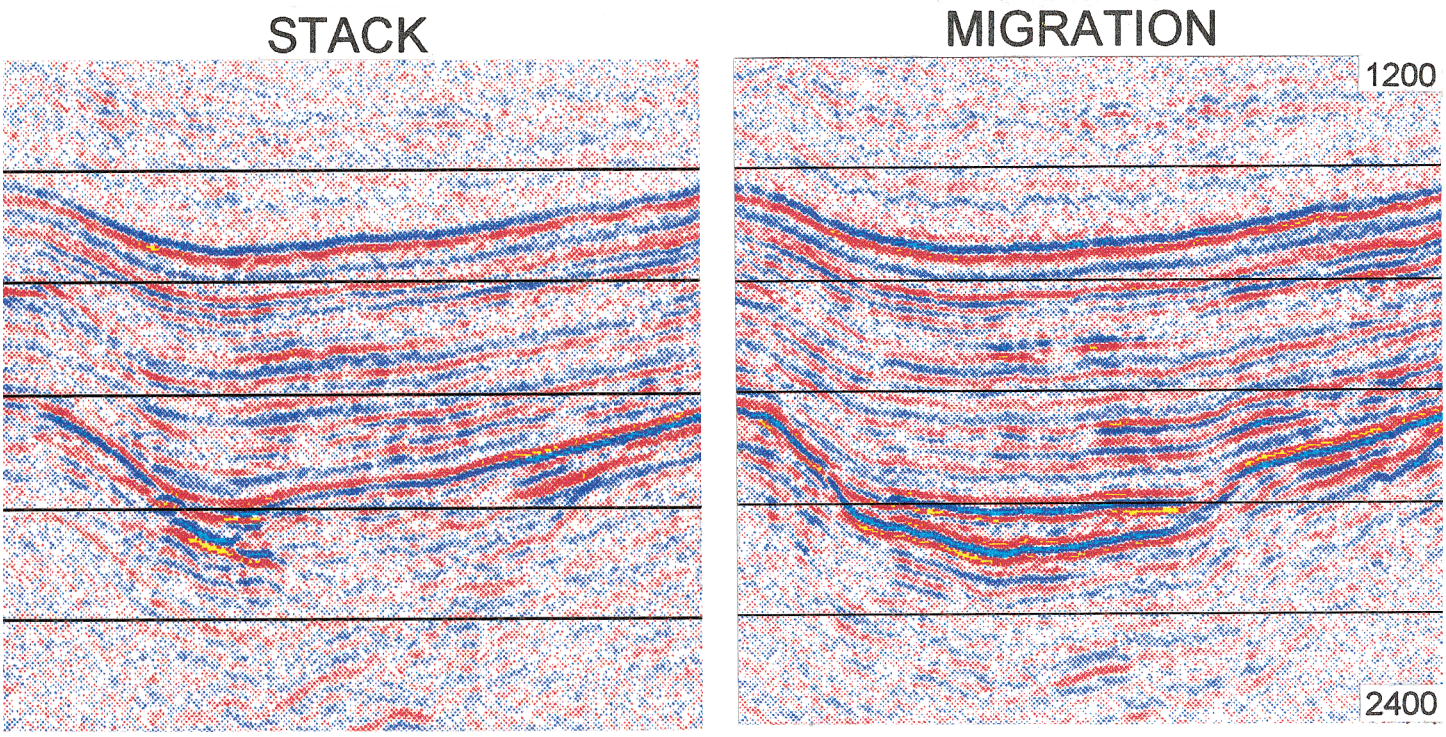

Fig. 1-14. Striking impact of 3-D migration on the attitude and continuity of reflections in South Australia. (Courtesy Santos Ltd.)

Table 1-3. Alias frequency (in hertz) as a function of subsurface spacing (in meters) and dip (in degrees) for an RMS velocity of 2500 m/s.

	SUBSURFACE SPACING				
DIP	12.5	25	50	75	100
5	574	287	143	96	72
10	288	144	72	48	36
15	193	96	48	32	24
20	146	73	37	24	18
25	118	59	30	20	15

Table 1-4. Basic formulas for the design of a 3-D survey.

Maximum subsurface spacing (2 samples per wavelength)	$= \frac{1}{2F_{max}\,DIP_{max}}$	where	T	is seismic two-way traveltime in seconds
Desirable subsurface spacing (3 samples per wavelength)	$= \frac{1}{3F_{max}\,DIP_{max}}$		DIP	is measured in seconds per unit distance
Migration distance (or half-aperture)	$= \frac{TV^2DIP}{4}$		F	is seismic frequency
Fresnel zone radius	$= \frac{V}{2}\sqrt{\frac{T}{F_{min}}}$		V	is seismic velocity

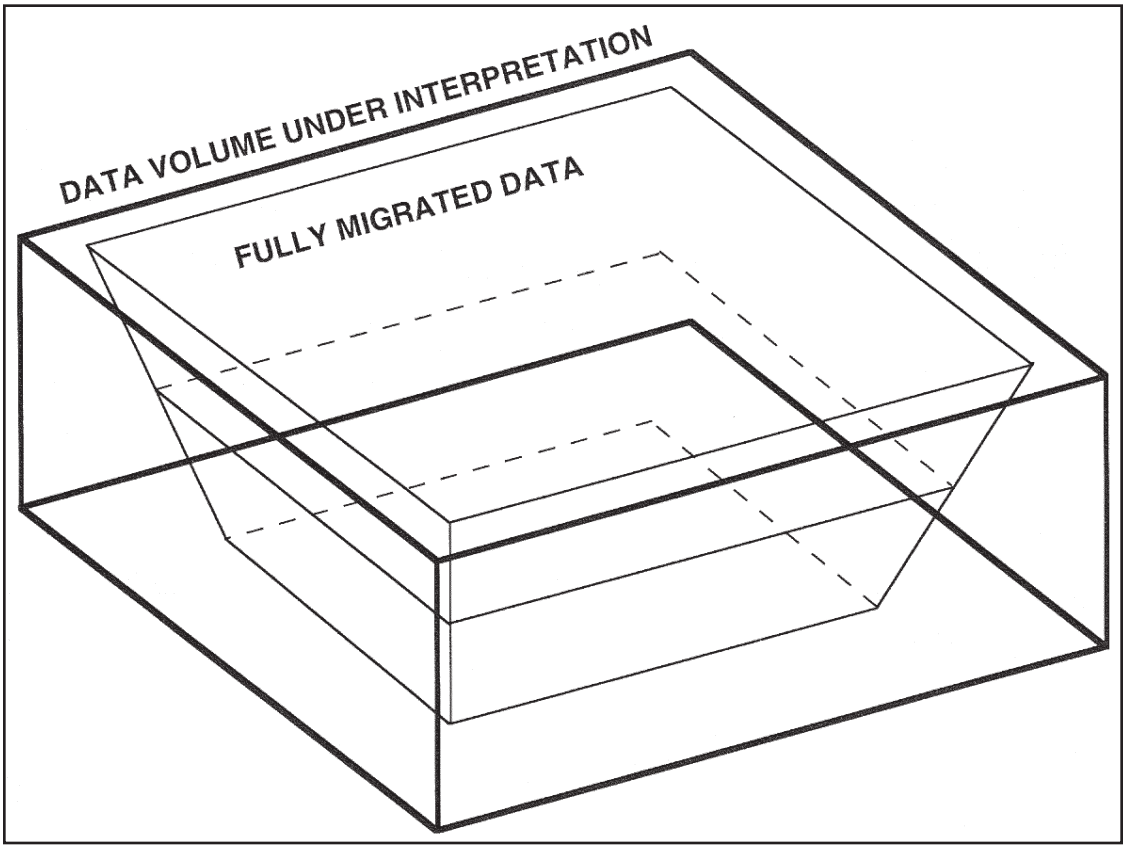

Fig. 1-15. Data around the edge of a 3-D survey are incompletely migrated because of migration distance and Fresnel zone radius. Interpreters should be extra cautious when working in this region.

overhang and provided valuable detail about traps located there against the salt face (Blake et al., 1982).

When comparing sections before and after 3-D migration to appraise its effectiveness, it is important to bear in mind the way in which reflections have moved around. In the presence of dip perpendicular to the section under scrutiny, the visible data before and after 3-D migration are different. It is unreasonable to compare detailed character and deduce what 3-D migration did. It is possible to compare a section before 3-D migration with the one from the same location after 3-D migration and find that a good quality reflection has disappeared. The migrated section is not consequently worse; the good reflection has simply moved to its correct location in the subsurface.

Figure 1-17 shows a horizontal section at a time of 224 ms from a very high resolution 3-D survey in Canada aimed at monitoring a steam injection process. The section on the left is from the 3-D volume before migration and the section on the right is from the volume after migration. The two black dots indicate wells. The striking visibility of a channel after migration results from the focusing of energy previously

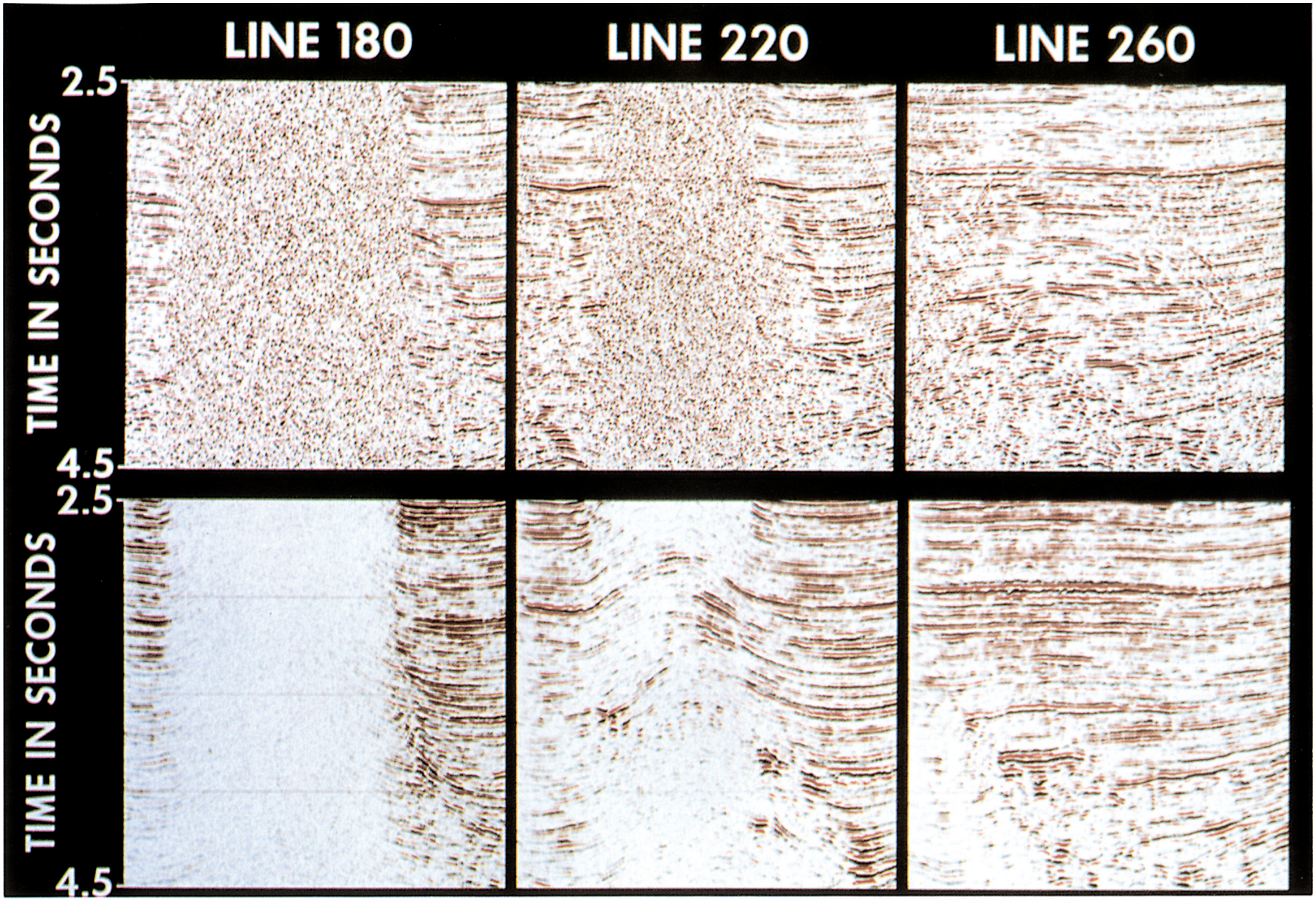

Fig. 1-16. Three vertical sections through or adjacent to a Gulf of Mexico salt dome before migration (top) and after migration (bottom), showing the repositioning of several reflections near the salt face. (Courtesy Hunt Oil Company.)

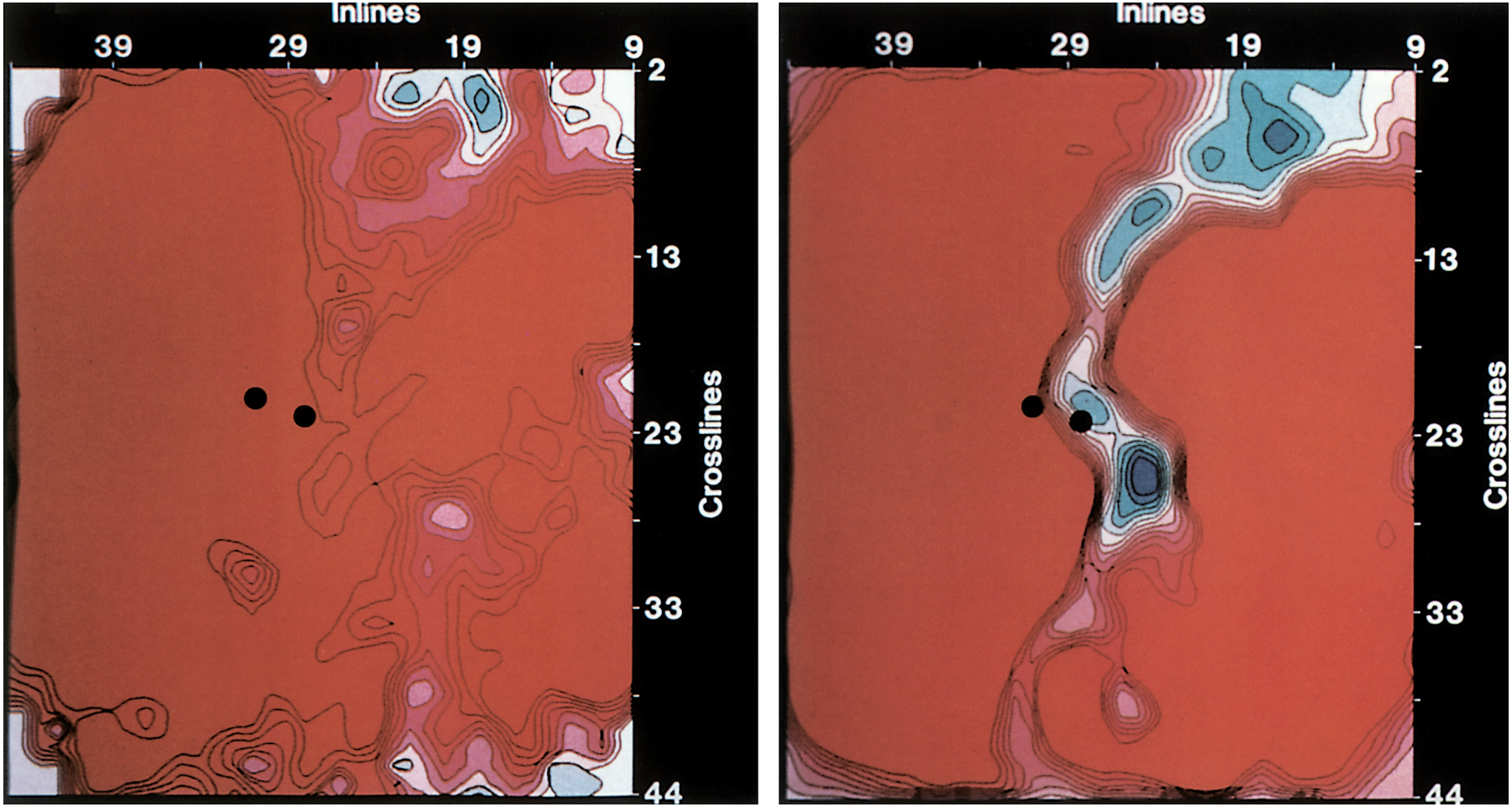

Fig. 1-17. Horizontal sections before migration (left) and after migration (right) showing the necessity of 3-D migration for the observation of shallow channels. (Courtesy Amoco Canada Petroleum Company Limited and N. E. Pullin.)

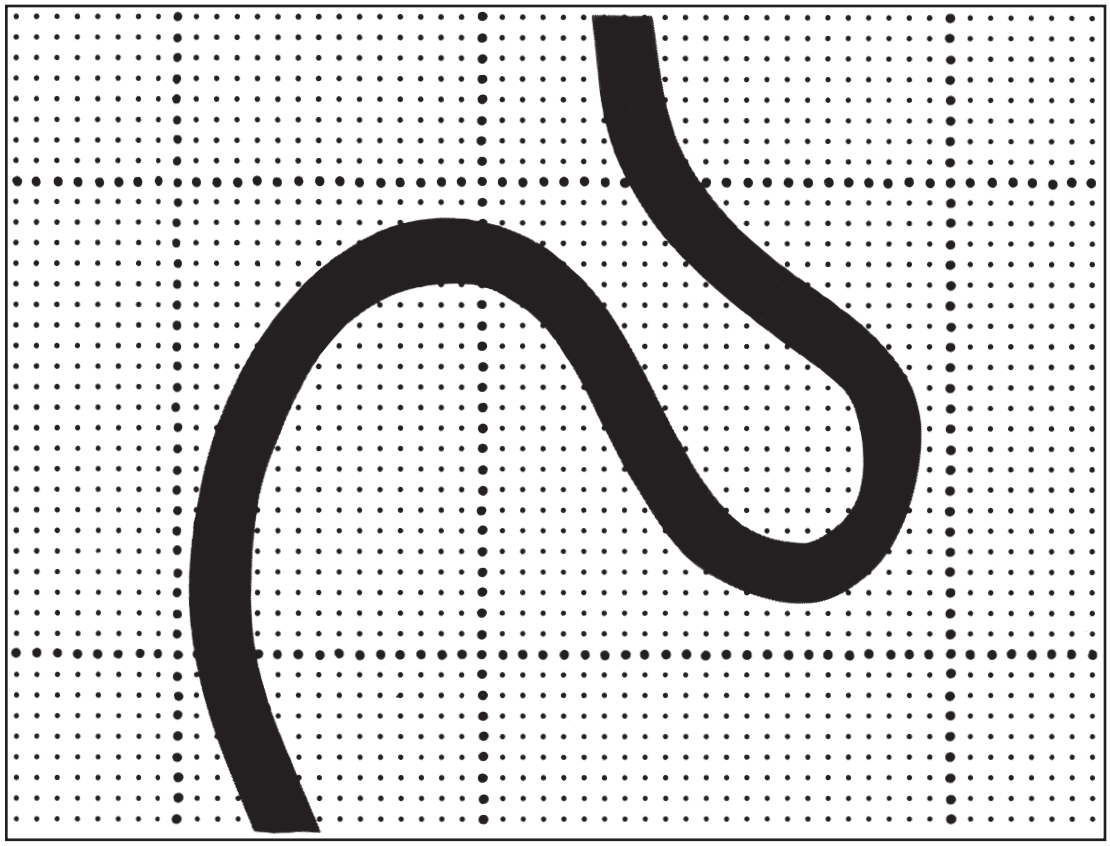

Fig. 1-18. Areal coverage of a 3-D survey compared to the coverage of a grid of five 2-D lines, and the ability of each to delineate a meandering channel.

spread over the Fresnel zone. The fact that one well penetrates the channel and the other does not is significant: they are only 10 m apart.

Survey Design

The sampling theorem requires that, for preservation of information, a waveform must be sampled such that there are at least two samples per cycle for the highest frequency. Since the beginning of the digital era, we have been used to sampling a seismic trace in time. For example, 4 ms sampling is theoretically adequate for frequencies up to 125 Hz. In practice we normally require at least three samples per cycle for the highest frequency. With this safety margin, 4 ms sampling is adequate for frequencies up to 83 Hz.

In space, the sampling theorem translates to the requirement of at least two, and preferably three, samples per shortest wavelength in every direction. In a normal 2-D survey layout this will be satisfied by the depth point spacing along lines but not by the spacing between lines. Hence the restriction that widely-spaced 2-D lines can be processed individually on a 2-D basis but not together as a 3-D volume.

If the sampling theorem is not satisfied the data are aliased. In the case of a dipping event, the spatial sampling of that event must be such that its principal alignment is obvious; if not, aliases occur and spurious dips result after multichannel processing. Table 1-3 shows the frequencies at which this aliasing occurs for various dips and subsurface spacings. Clearly, a 3-D survey must be designed such that aliasing during processing does not occur. Tables like the one presented can be used to establish the necessary spacing considering the dips and velocities present. In order to impose the safety margin of three samples, rather than two, per shortest wavelength, the frequency limit is normally considered to be around two-thirds of each number tabulated. The formulas in Table 1-4 provide a general method of establishing the spacings required. The first formula, based on two samples per shortest wavelength, gives the maximum

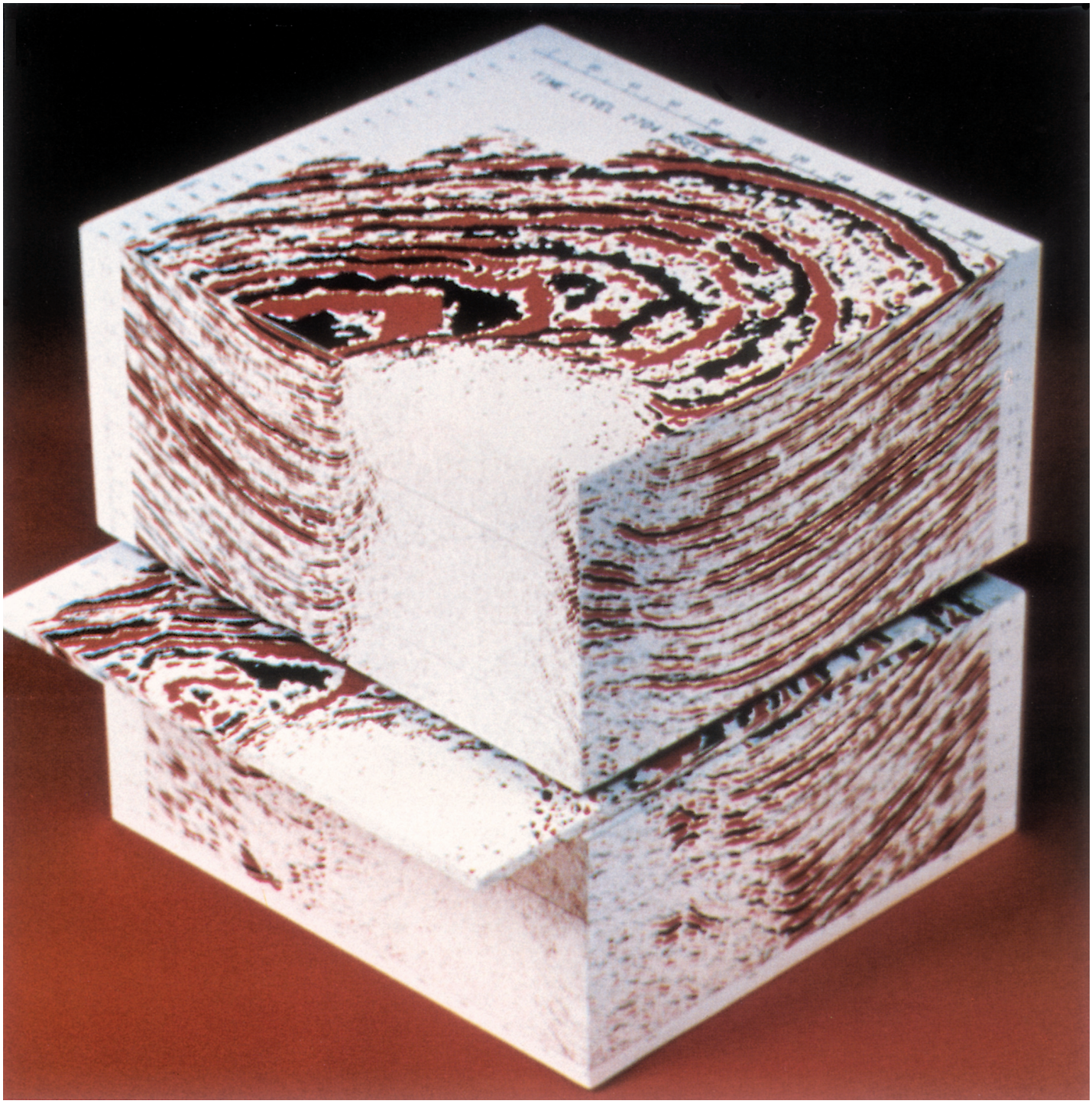

Fig. 1-19. 3-D data volume showing a Gulf of Mexico salt dome and associated rim syncline. (Courtesy Hunt Oil Company).

spacing that can be used to image the structure. Given our ignorance of the subsurface structure at the time the 3-D survey is being designed, we should allow a significant safety margin by collecting at least three samples per shortest spatial wavelength.

Table 1-4 also shows the two formulas needed to calculate the width of the extra strip around the periphery of the prospect over which data must be collected in order to ensure proper imaging in the area of interest. The calculation of migration distance, the extra fringe width needed for structure, should use the local value of dip measured perpendicular to the prospect boundary. The Fresnel zone radius, the extra fringe width needed for stratigraphy, needs to be considered for the proper focusing of amplitudes. The two strip, or fringe, widths thus calculated should be added

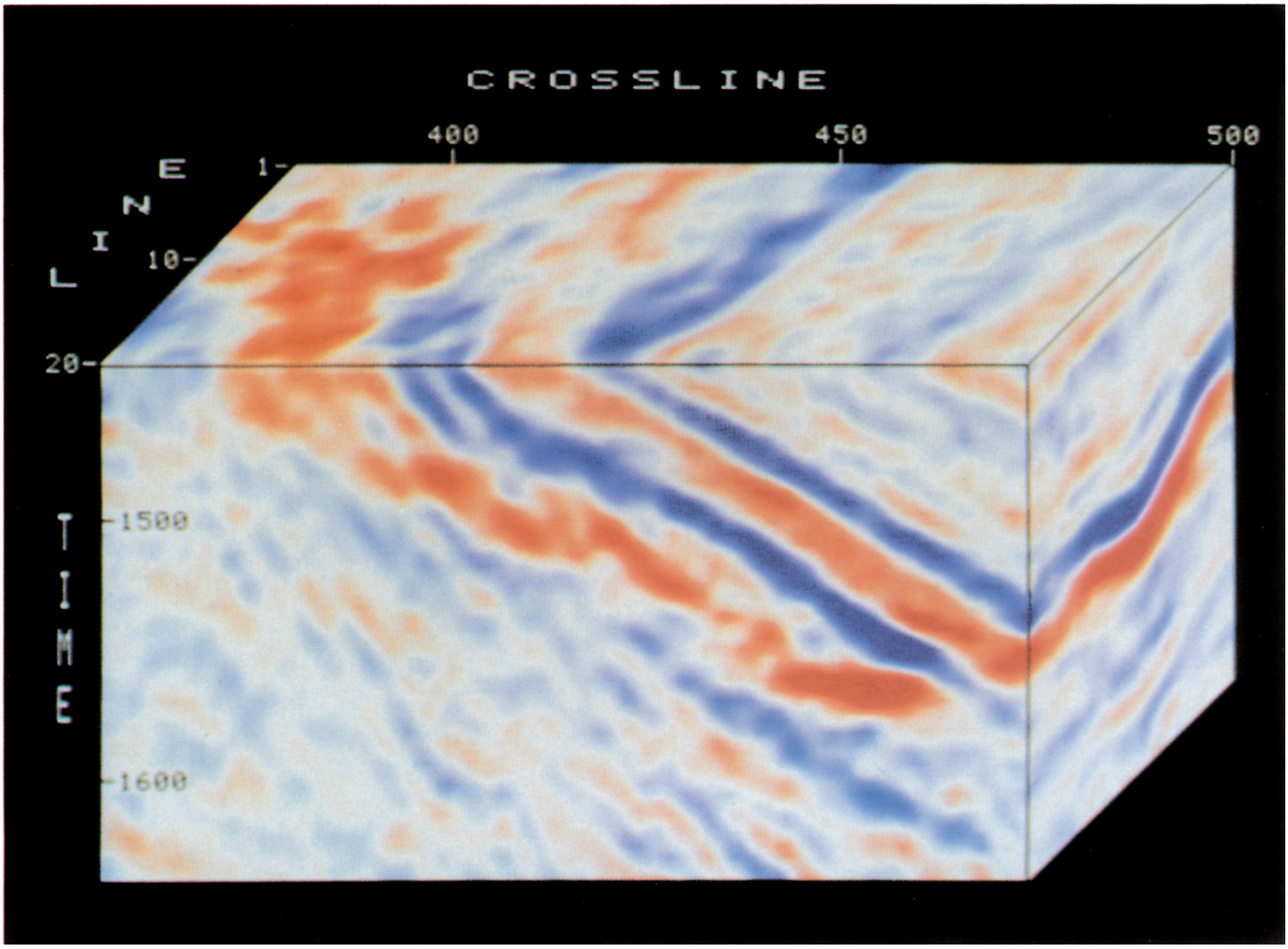

Fig. 1-20. 3-D data volume showing a bright spot from a Gulf of Mexico gas reservoir. (Courtesy Chevron U.S.A. Inc.)

together in defining the total survey area.

A typical 3-D seismic interpreter does not get involved in designing surveys but nevertheless needs to appreciate these issues. Figure 1-15 demonstrates that, of the data volume under interpretation, only the central portion is fully migrated and therefore fully reliable. The fringe between the inner and outer volumes is the migration distance and the Fresnel zone radius. If the interpreter is working in this fringe zone he needs to realize that the data are unreliable and the results are subject to greater risk.

Proper design of a 3-D survey is critical to its success, and sufficiently close spacing is vital. The formulas of Table 1-4 are addressing structural design issues. In areas of shallow dip where the survey objectives are stratigraphic, the selected spacing must be such that there are at least two samples within the lateral extent of any expected stratigraphic feature of interest, for example the width of a channel. Figure 1-18 demonstrates a typical comparison between the subsurface sampling of a 2-D and 3-D survey. The bold dots indicate the 2-D survey depth points which satisfy the sampling theorem along each line. The 3-D survey requires a similarly close spacing in both directions over the whole area. In addition to the opportunity for three-dimensional processing which the areal coverage provides, note the sampling and thus potential definition of a meandering stream channel. Sampling for stratigraphic features like this channel requires at least two but preferably three samples within the channel width. In practice, 3-D depth point spacing ranges between 6 and 50 m.

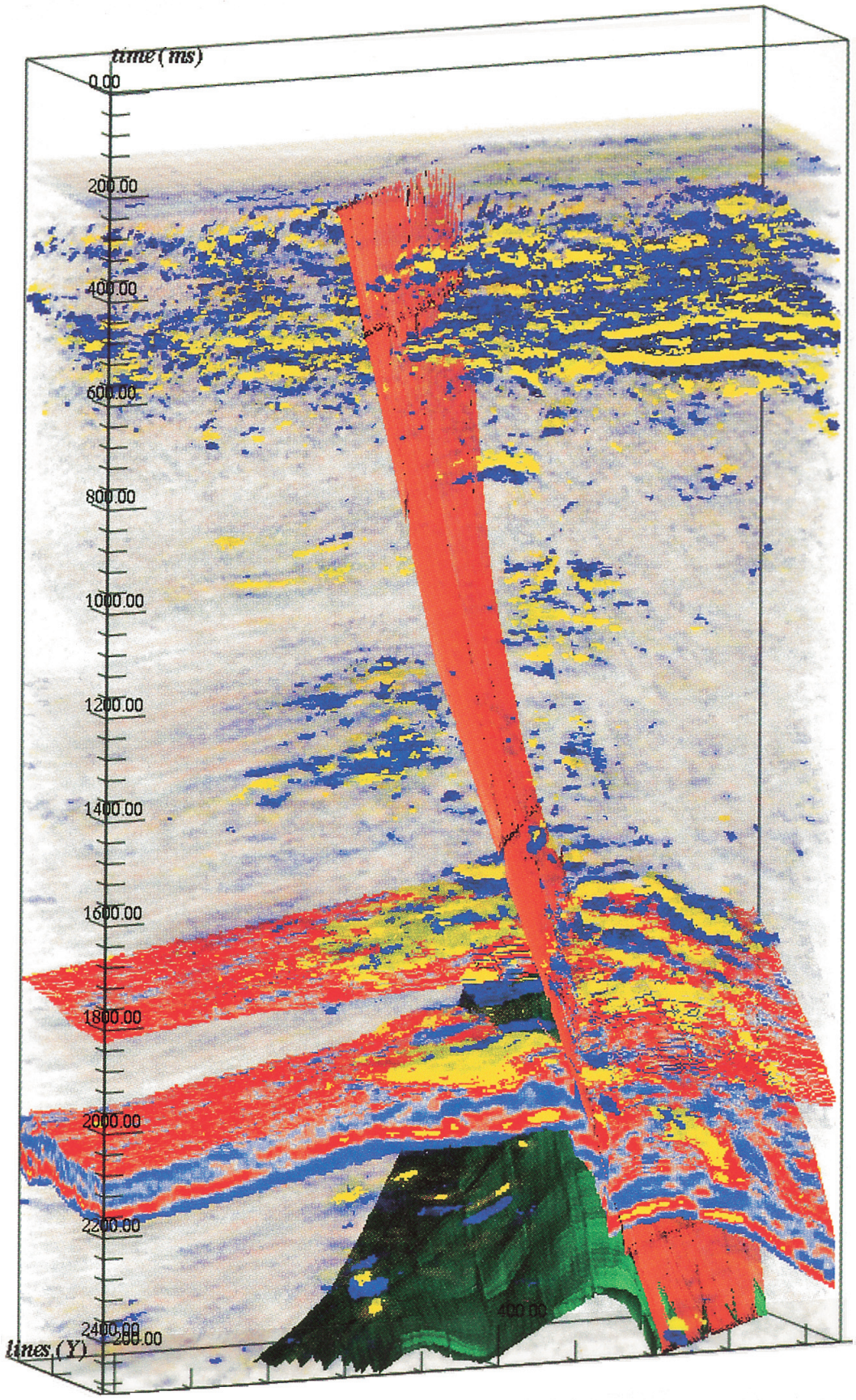

Fig. 1-21. Voxel-rendered view of data volume which, by making the voxels semi-transparent, permits the interpreter to look into the volume. (Courtesy CogniSeis Development.)

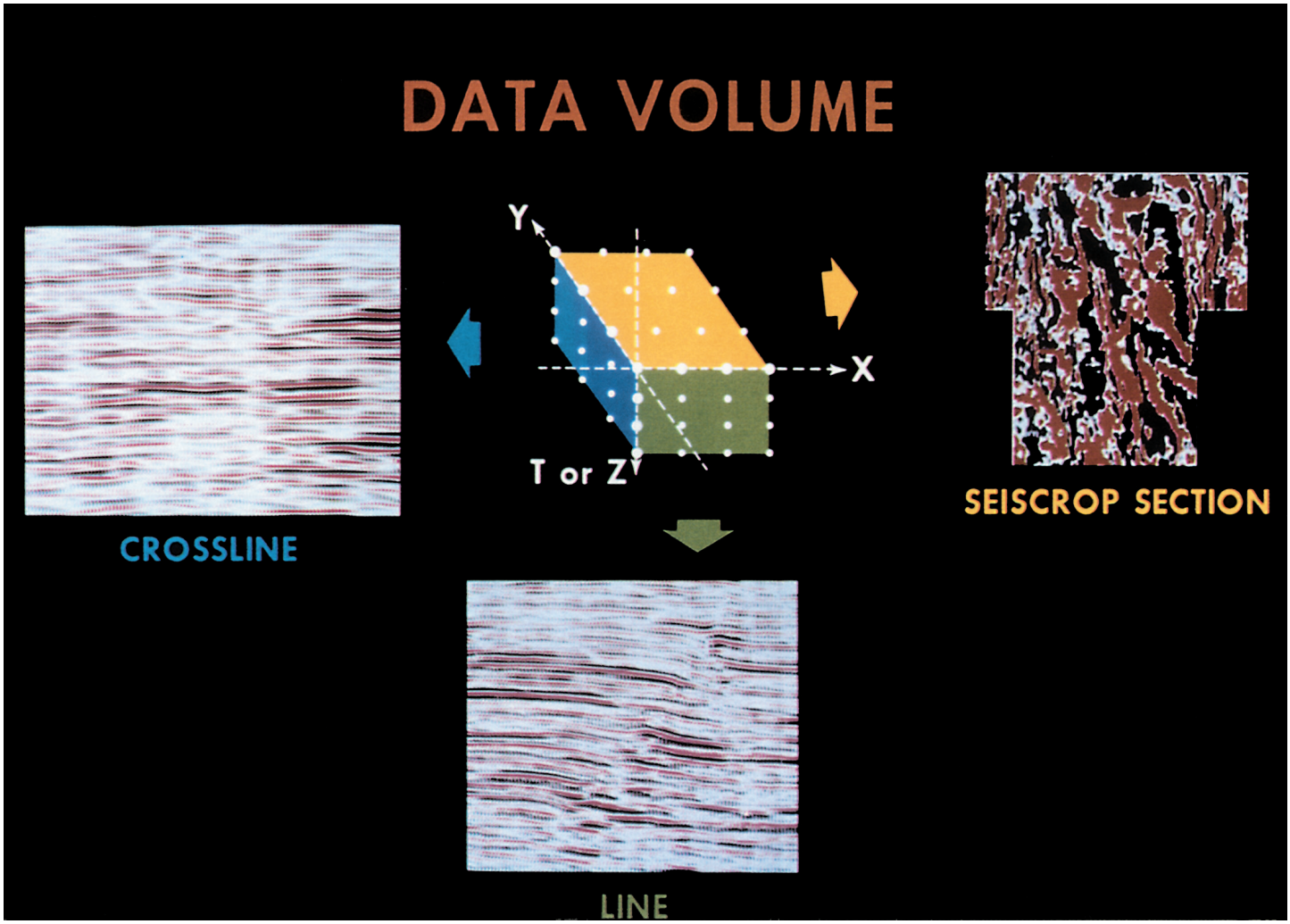

Fig. 1-22. Three sets of orthogonal slices through a data volume provide the basic equipment of the 3-D seismic interpreter.

Volume Concept

Collection of closely spaced seismic data over an area permits three-dimensional processing of the data as a volume. The volume concept is equally important to the seismic interpreter. With 3-D data, the interpreter is working directly with a volume rather than interpolating a volumetric interpretation from a widely-spaced grid of observations. The handling of this volume and what can be extracted from it are principal subjects of this book. One property of the volume pervades everything the 3-D interpreter does: The subsurface seismic wavefield is closely sampled in every direction, so that there is no grid loop around which the interpreter must tie, and no grid cell over which he must guess at the subsurface structure and stratigraphy. This is an opportunity which an interpreter must use to full advantage. Because the sampling requirements for interpretation are the same as for processing, all the processed data points contain unique information and thus should be used in the interpretation. Thus, the interpreter of a 3-D volume should not decimate the data available to him but, given that he has time constraints imposed on him, he should use innovative approaches with horizontal sections, specially selected slices, and automatic spatial tracking, in order to comprehend all the information in the data. In this way the 3-D

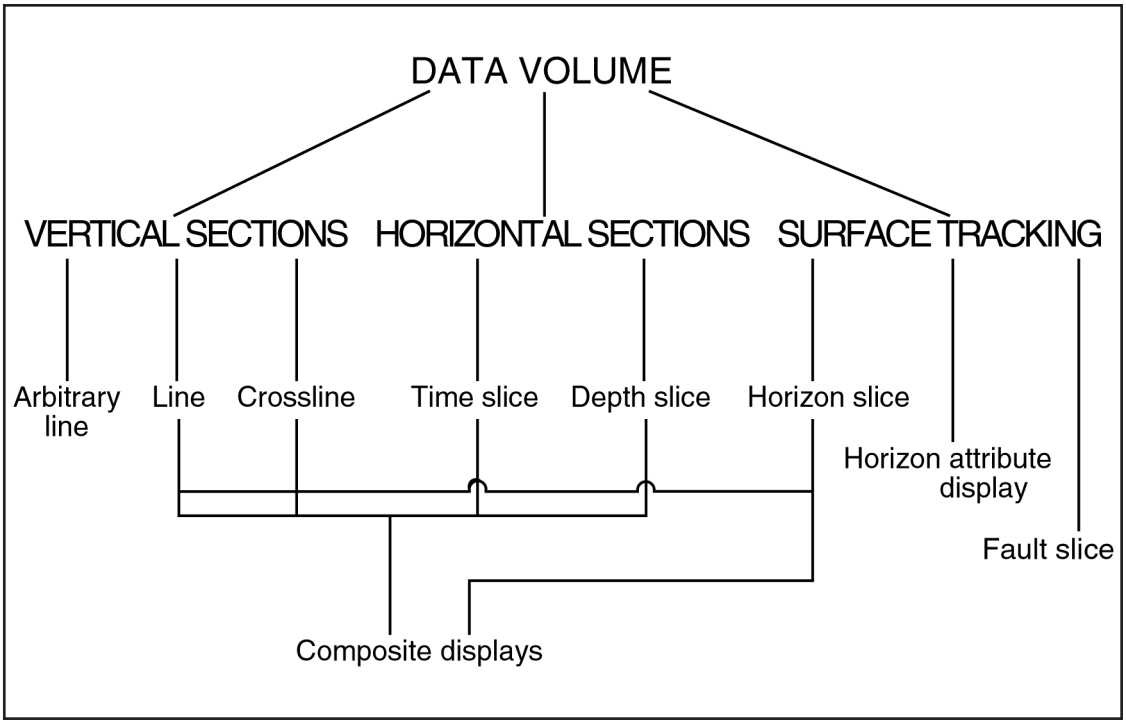

Fig. 1-23. Recognized and approved terms for display products from 3-D seismic data. All display seismic amplitude unless specified otherwise. Use of all other terms should be discouraged.

seismic interpreter will generate a more accurate and detailed map or other product than his 2-D predecessor in the same area.

Figure 1-19 shows a view of a 3-D data volume through a salt dome. It demonstrates the volume concept well and the interpreter can use a display of this kind to help in appreciation of subsurface three-dimensionality. Figure 1-20 shows another cube, in this case generated interactively, which helps in the three-dimensional appreciation of a much more detailed subsurface objective. Neither of these displays, however, permits the interpreter to look *into* the volume of data.

True 3-D display has recently become a reality on computer workstations and Figure 1-21 shows an example. The portion of the volume being displayed is composed of voxels, or volume elements, and these are rendered with differing degrees of transparency so that the interpreter can really see into the volume. In Figure 1-21 there are four interpreted surfaces as well as the semi-transparent data. As with any volumetric display the dynamic range is reduced because of the quantity of data viewed. These types of display are very useful for data visualization but they are not yet fully integrated into mainstream interpretation systems.

Slicing the Data Volume

The majority of 3-D interpretation is performed on slices through the data volume. There are no restrictions on the dynamic range for the display of any one slice, and therefore all the benefits of color, can be exploited (see Chapter 2). The 3-D volume contains a regularly-spaced orthogonal array of data points defined by the acquisition geometry, and maybe adjusted during processing. The three principal directions of the array define three sets of orthogonal slices or sections through the data, as shown in Figure 1-22.

The vertical section in the direction of boat movement or cable lay-out is called a **line** (sometimes an **inline**). The vertical section perpendicular to this is called a **crossline**. The horizontal slice is called a **horizontal section, time slice**, **or depth slice**. The terminology used for slices through 3-D data volumes has become somewhat confused. One of the objectives of this chapter is to clarify terms in common use today.

Three sets of orthogonal slices through the data volume (as defined above) are regarded as the basic equipment of the 3-D interpreter. A complete interpretation will

Fig. 1-24. An early optical workstation.

make use of some of each of them. However, many other slices through the volume are possible. A **diagonal line** may be extracted to tie two locations of interest, such as wells. A zig-zag sequence of diagonal line segments may be necessary to tie together several wells in a prospect. In the planning stages for a production platform, a diagonal line may be extracted through the platform location along the intended azimuth of a deviated well. All these are vertical sections and are referred to as **arbitrary lines**.

More complicated slices are possible for special applications. A slice along or parallel to a structurally interpreted horizon, and hence along one bedding plane, is a **horizon slice.** Slices of this kind have particular application for stratigraphic interpretation, which is explored in Chapter 4. **Fault slices** generated parallel to a fault face have various applications in structural and reservoir interpretation and will be discussed in Chapter 7. **Horizon attribute displays** are the subject of Chapter 8.

Figure 1-23 shows a hierarchy of approved terms for display products from 3-D seismic data. It shows, for example, the equivalence of horizontal and vertical sections, and the equivalence of time slices with lines and crosslines. In order to aid worldwide communication, use of other terms is discouraged.

Workstations

In the early days of 3-D interpretation a sequence of horizontal sections was displayed on film-strip and shown as a motion picture (Bone, Giles, and Tegland, 1983).

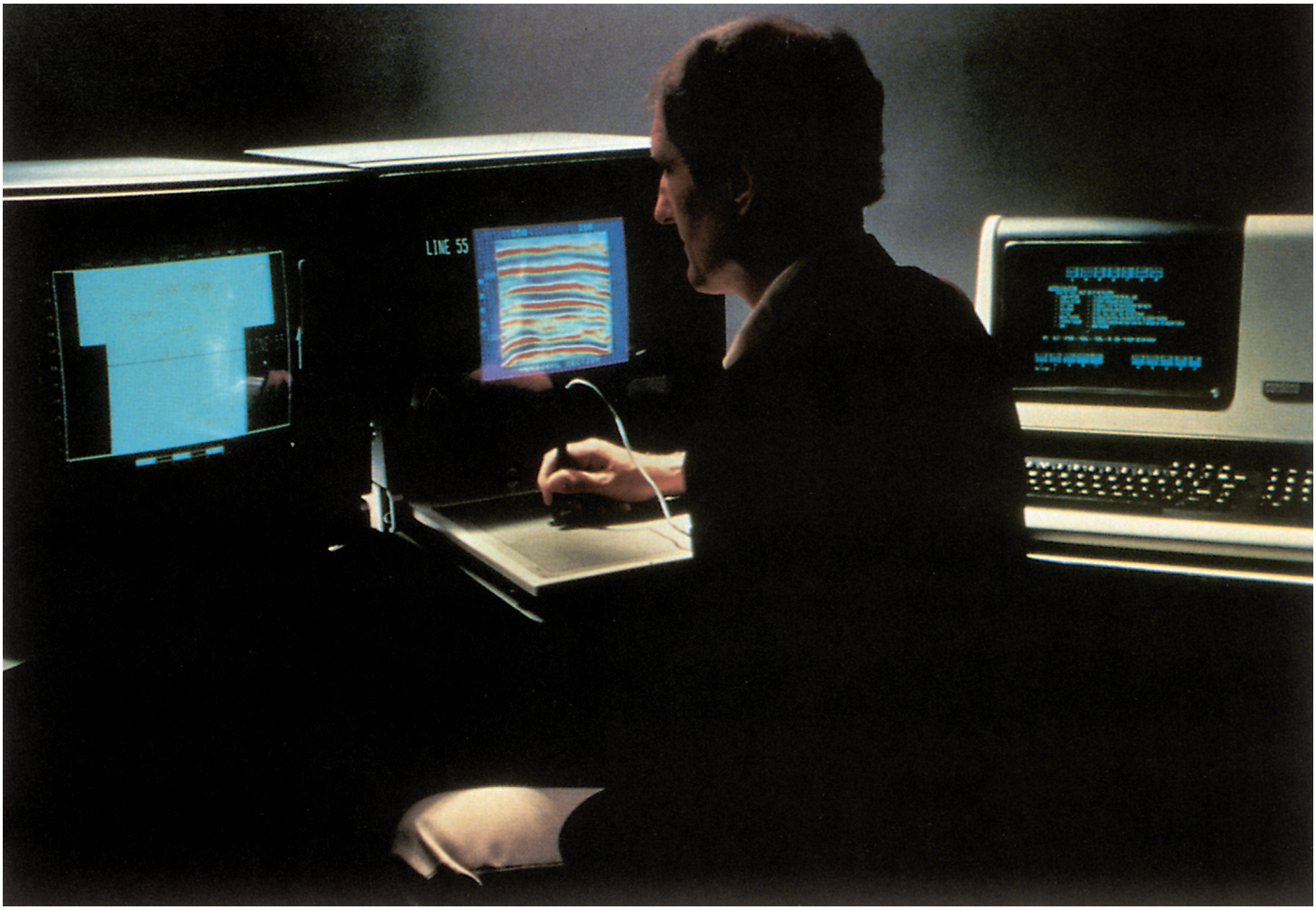

Fig. 1-25. An early interactive workstation.

From this developed the Seiscrop Interpretation Table — initially a commercially-available piece of equipment incorporating a 16mm analytical movie projector. This machine was originally developed for coaches wanting to examine closely the actions of professional athletes.

The Seiscrop Interpretation Table then evolved into a custom-built device (Figure 1-24). The data, either horizontal or vertical sections, were projected from 35mm film-strip onto a large screen. The interpreter fixed a sheet of transparent paper over the screen for mapping and then adjusted the size of the data image, focus, frame advance, or movie speed by simple controls.

Today 3-D interpretation is performed interactively and there has been an explosion in workstation usage in recent years. The interpreter calls the data from disk and views them on the screen of a color monitor (Figure 1-25). The large amount of regularly-organized data in a 3-D volume gives the interactive approach enormous benefits. In fact, many interactive interpretation systems addressed 3-D data first as the easier problem, and then developed 2-D interpretation capabilities later.

Most of the interpretation discussed in this book resulted from use of an interactive workstation, and many of the data illustrations are actual screen photographs. Furthermore, the facilities of the system contributed in several significant ways to the success of many of the projects reported here. Hence it is appropriate to review the interpretive benefits of an interactive interpretation system.

(1) **Data management** — The interpreter needs little or no paper; the selected seismic data display is presented on the screen of a color monitor and the progressive results of interpretation are returned to the digital database.

(2) **Color** — Flexible color display provides the interpreter with maximum optical dynamic range adapted to the particular problem under study.

(3) **Image composition** — Data images can be composed on the screen so that the interpreter views what is needed, no more and no less, for the study of one particular issue. Slices through the data volume are designed by the user in order to customize the perspective to the problem.

(4) **Idea flow** — The rapid response of the system makes it easy to try new ideas. The interpreter can rapidly generate innovative map or section products in pursuit of a better interpretation.

(5) **Interpretation consistency** — The capability to review large quantities of data in different forms means that the resulting interpretation should be more consistent with all available evidence. This is normally considered the best measure of interpretation quality.

(6) **More information** — Traditional interpretive tasks performed interactively will save time; however, the extraction of more detailed subsurface information is more persuasive and far-reaching.

Dynamic Range and Data Loading

Interactive interpretation must commence with data loading and this is a critical first step. Data processing has always been performed using 32 bits to describe each amplitude value. This large word size ensures that significance is retained during all computations. The first interactive systems in the early 1980s were 32-bit machines but soon a demand for speed dictated that data be loaded using 8 bits only. The small word reduces response time and minimizes storage space for the survey data. Today interactive systems offer a choice of 8-bit, 16-bit, or 32-bit dynamic range, although color monitors normally display 8 bits only.

Figure 1-26 shows a typical statistical distribution of amplitudes in a data volume. There are a large number of very low amplitudes, a fairly large number of moderate amplitudes but a very small number of high amplitudes. Mainstream structural interpretation tends to work on moderate amplitude horizons. The high amplitude tails of the distribution are localized anomalies which, in tertiary clastic basins, are often the hydrocarbon bright spots. The interpreter avoids the low amplitudes as much as possible because they are the most subject to noise. Thus most interpretive time is devoted to the amplitudes lying in the stippled areas of Figure 1-26.

If interpretation is to be conducted using 8 bits only, scaling 32-bit amplitude numbers to 8-bit amplitude numbers must be done during data loading. If the maximum amplitude in the volume is set to ± 128, relative amplitudes are preserved within the precision of the 8 bits. However, this often severely limits the dynamic range available in the stippled, or heavily used, amplitude regions. Clipping of the highest amplitudes is a common reaction to this problem so that a smaller value is set to ±128. More dynamic range is then available for the mainstream structural interpretation but the highest amplitudes are destroyed and hence unavailable for stratigraphic or reservoir analysis. This can be very damaging particularly in areas like the Gulf of Mexico. Some interactive workstations load 8-bit data with a floating point scalar defined individually for each trace and stored in the trace header. This lessens but does not remove the dynamic range problem discussed above.

A common and generally desirable solution today is to load the data using 16 bits for each amplitude value. In this way clipping is irrelevant and unnecessary. There is plenty of dynamic range for structural interpretation *and* bright spot studies, because amplitude values available with 16 bits cover the range ± 32,768.

An interesting comparison of 8-bit and 16-bit interpretation was conducted by Roberts and Hughes (1995). They concluded that there are always differences between interpretation products from 8-bit and 16-bit volumes but they are generally less than 5%. These may or may not be tolerable, and they stressed the need for *sensible clipping*. Figure 1-27 is a test for and demonstration of data clipping. Contrasting colors have been placed in the extremities of the otherwise-gradational color scheme. The large

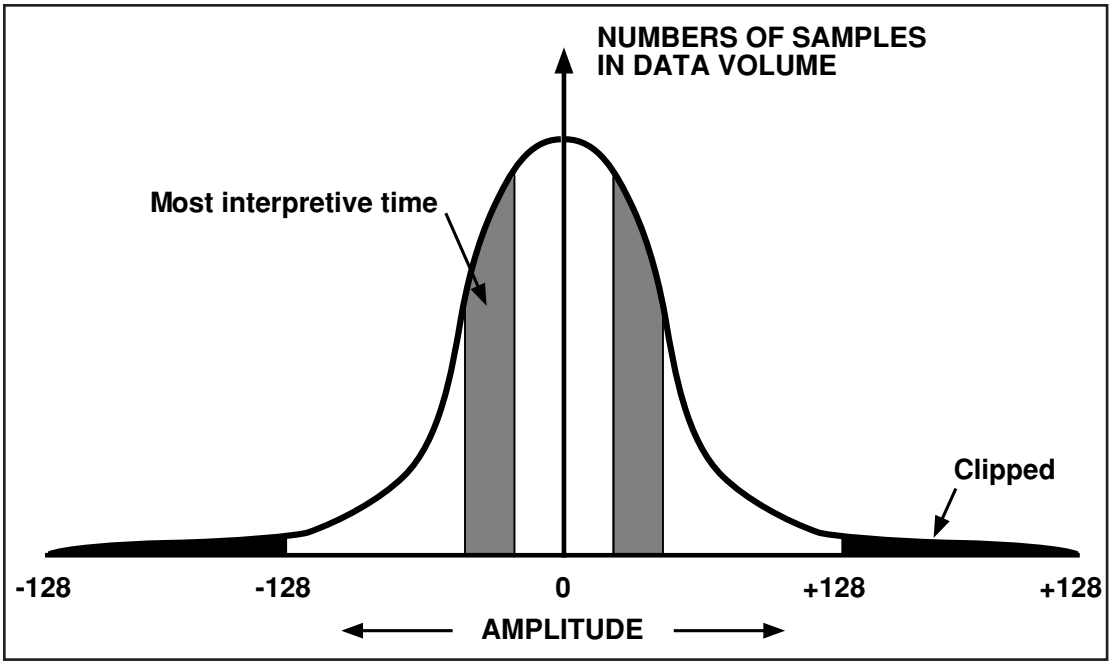

Fig. 1-26. Typical statistical distribution of amplitudes in a 3-D data volume. Plus or minus 128, the largest number which can be described by 8 bits, may be set to the largest amplitude, or alternatively to some smaller amplitude, thus causing data clipping.

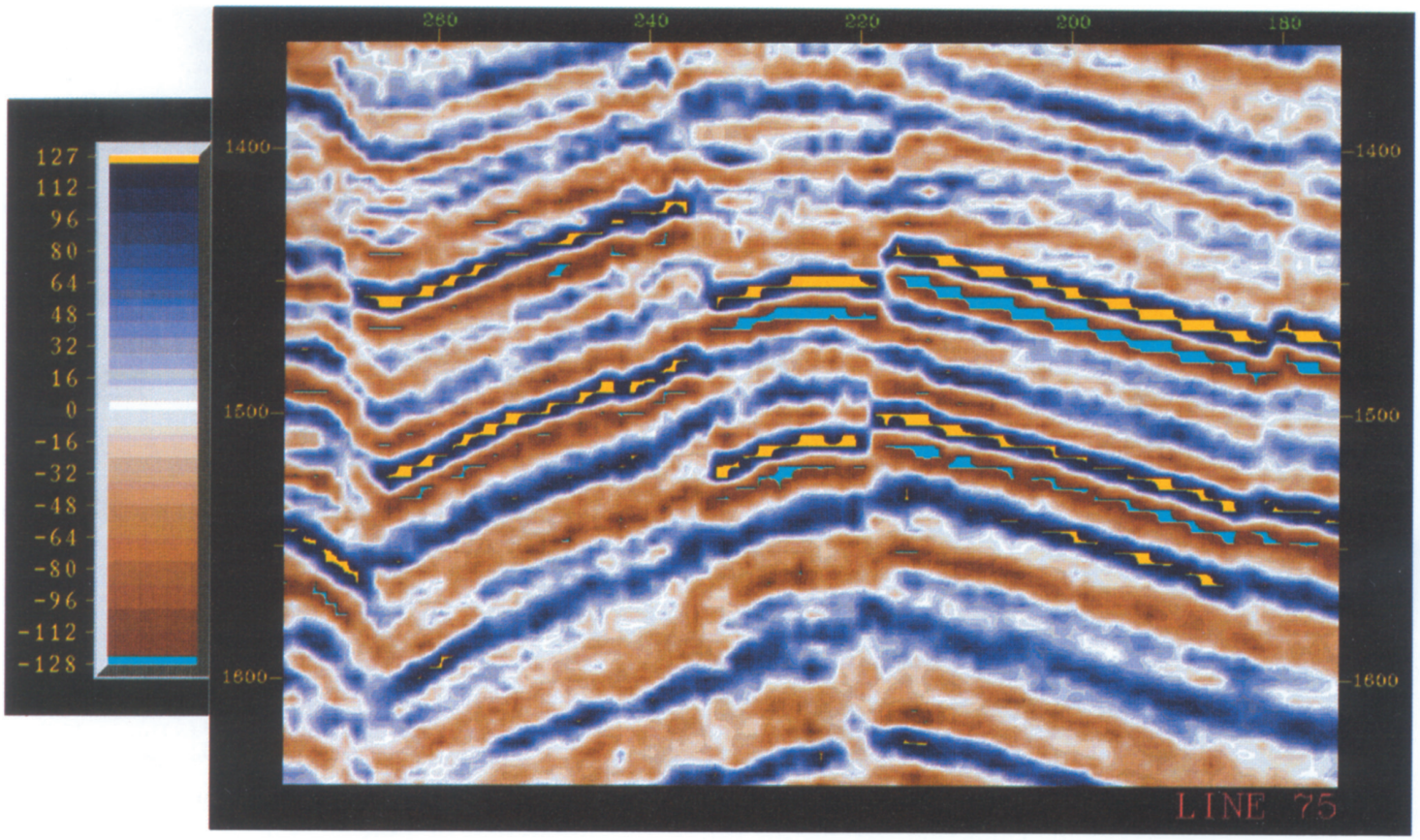

Fig. 1-27. Test for and demonstration of data clipping.

amounts of yellow and cyan demonstrate an anomalously high occupancy of those highest amplitudes, that is the data has been heavily clipped.

The author is opposed to data clipping as it places restrictions on interpretation activities. Generally the best solution is to use 16 bits and sometimes 32 bits. The total interpretation project today often involves a significant amount of post-interpretation computation. The larger number of bits helps ensure that numeric significance is maintained during these operations. Fortunately faster and cheaper hardware is now available which makes the use of 16 or 32 bits much less of a burden than it was in the past.

Acquisition Footprint

Seismic data acquisition and processing should be conducted in a very regular manner. We want to interpret visible irregularities in the data in terms of geology; we do not want spatial irregularities in the data to indicate the variations in the acquisition or processing operation. Ideally, we would like every bin to be filled with the same number of recorded traces with the same offset distribution and with the same azimuth distribution. However, this is impossible to achieve within a reasonable budget. If any or all of the recording parameters vary in some spatially systematic way, then the data acquisition geometry is commonly visible in the data as a footprint. Cordsen, Galbraith, and Peirce (2000) discuss various acquisition geometries and the many causes of footprint.

Figure 1-28 shows a severe footprint on a horizon slice extracted from land data. Shot lines and receiver lines are typically laid out perpendicular to each other on land (left), causing the gridlike pattern in amplitude (right). Marine data typically have a linear footprint aligned in the direction of boat movement. Figure 1-29 shows a mild marine footprint and a channel system. Footprint is difficult to predict, is more apparent at shallow depths, is generally expensive to eliminate in the field, and is complicated to remove in data processing. Interpreters need to be alert to footprint so that they do not confuse it with stratigraphic patterns. The horizon slice, the most important display for stratigraphic interpretation (Chapter 4), is particularly sensitive to footprint. Often an interpreter observes footprint in his data when he sees the first horizon slice, and this is the very time he wishes he didn't have the problem.

Difficulties of survey access caused by obstacles or no-permit zones lead to gaps in surface coverage and thus to an irregular footprint effect. Interruptions in surface coverage can cause amplitude terminations at depth which can be confused with stratigraphic boundaries. Figure 1-30 shows a red-over-blue amplitude objective high on structure which at first sight looks prospective. However, the severe lack of surface coverage on the right reduces amplitude for all reflections and thus reduces confidence that the amplitude objective has a geologic cause. Figure 1-31 is similar. The very strong hydrocarbon amplitude on the right at depth is greatly attenuated on the left because of surface effects.

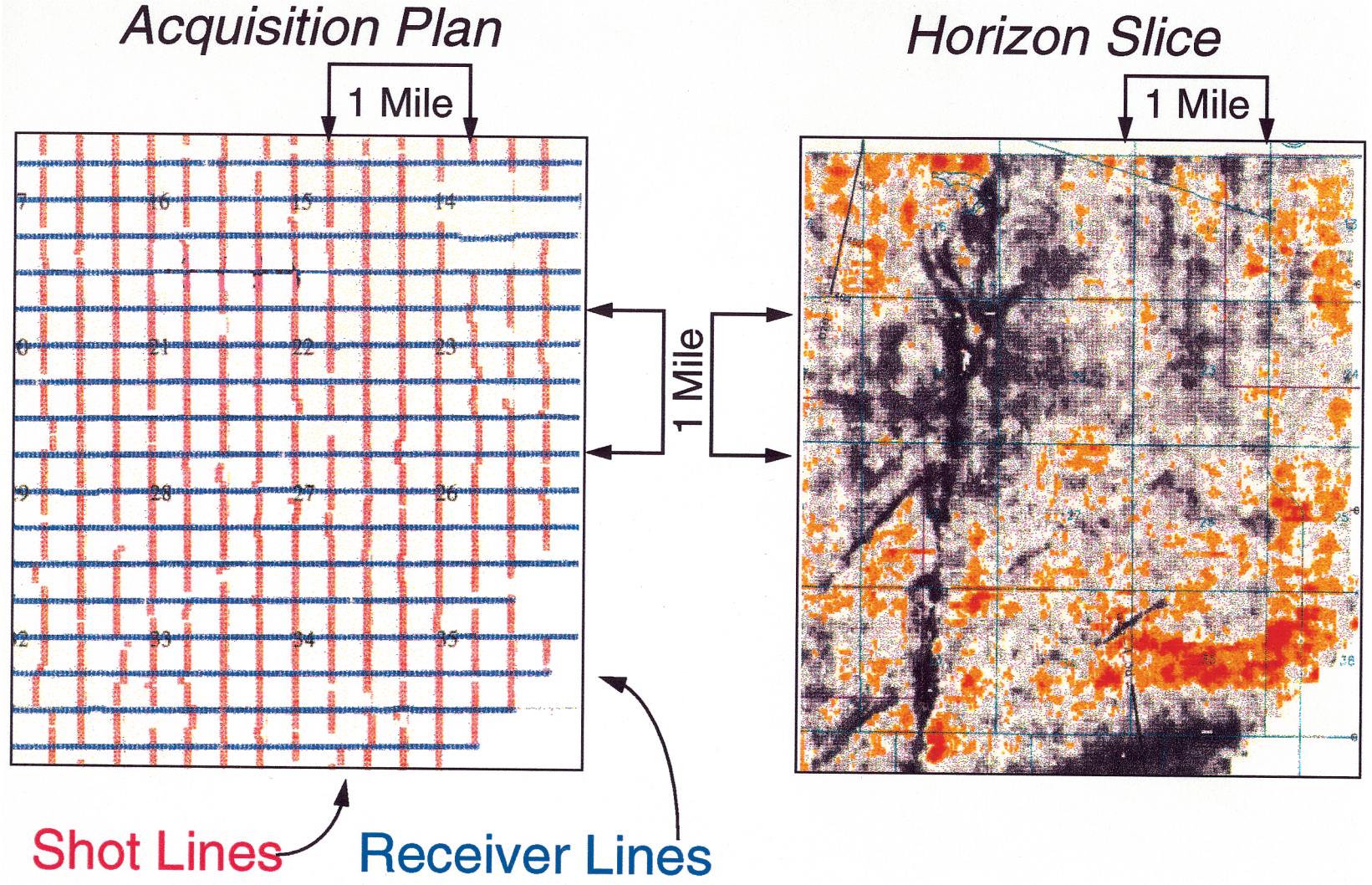

Fig. 1-28. Acquisition footprint is the imprint of the data acquisition geometry on horizon slices and similar areal displays. Example of a severe footprint for a land survey. (Courtesy Amoco Production Company.)

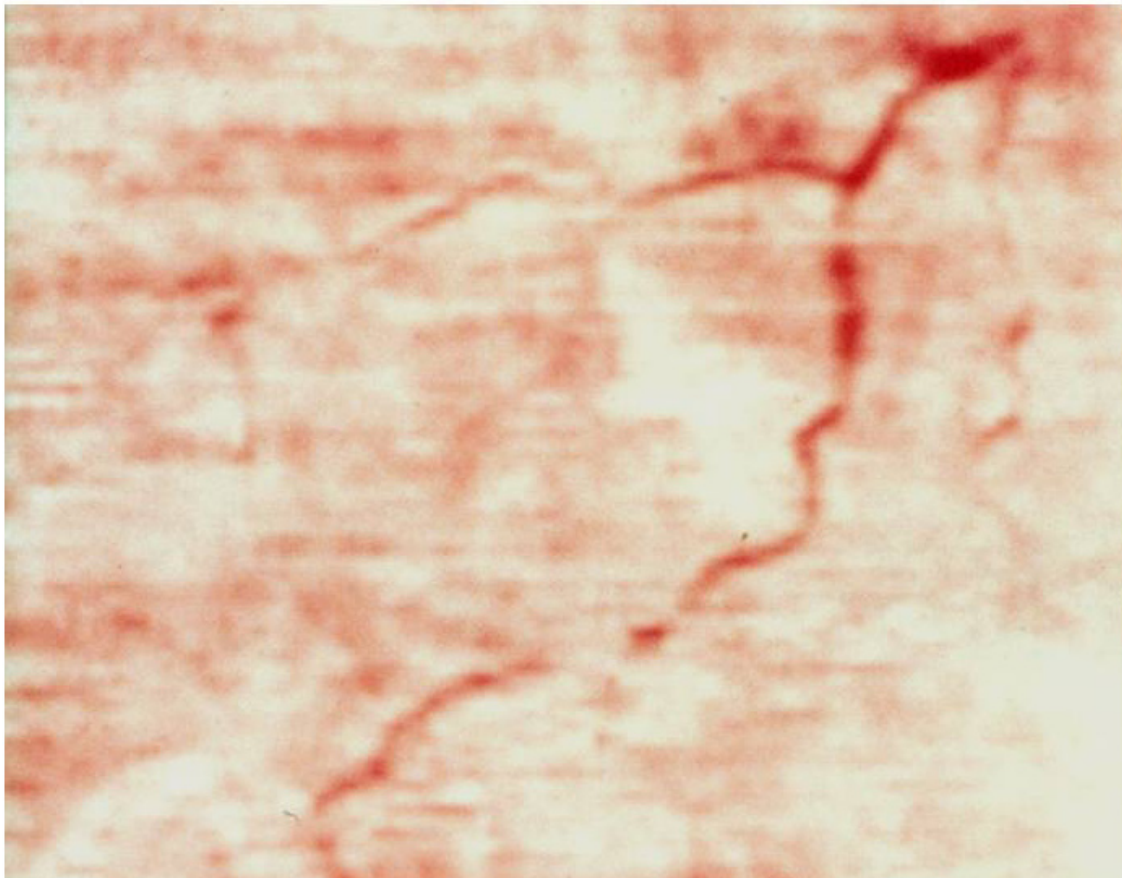

Fig. 1-29. Footprint in marine data. Note mild lineations running left to right.

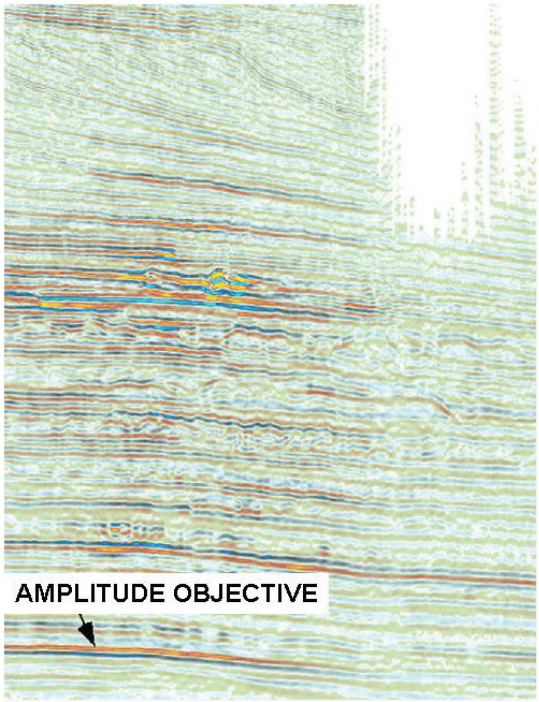

Fig. 1-30. Amplitude objective appears less prospective because all amplitudes on right are reduced by low surface coverage (after Sheriff et al., 2010; used by permission of the Society of Exploration Geophysicists). (Courtesy Pemex.)

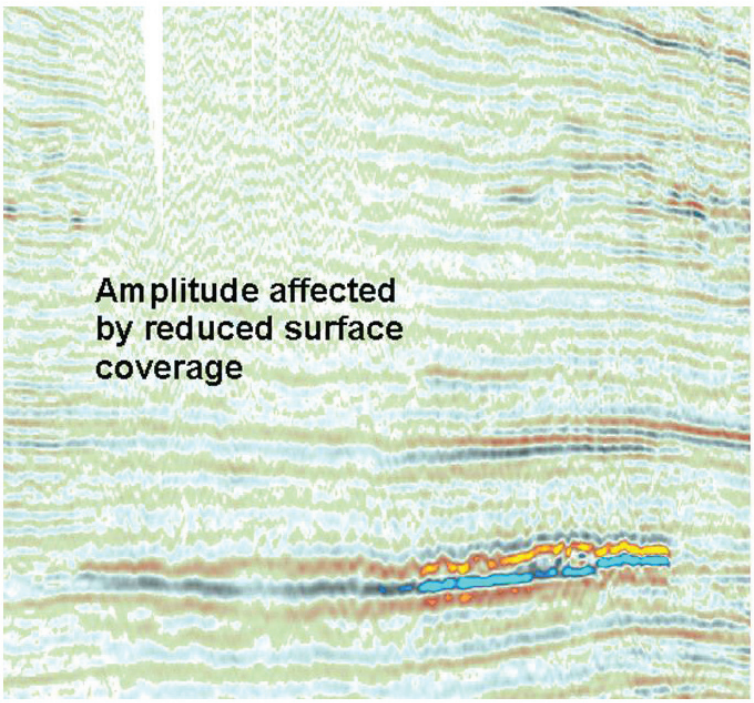

Fig. 1-31. Known hydrocarbon amplitude severely affected on left by reduced surface coverage. (Courtesy Pemex.)

References

Blake, B. A., J. B. Jennings, M. P. Curtis, and R. M. Phillipson, 1982, Three-dimensional seismic data reveals the finer structural details of a piercement salt dome: Offshore Technology Conference paper 4258, p. 403–406.

Bone, M. R., B. F. Giles, and E. R. Tegland, 1976, 3-D high resolution data collection, processing and display: Houston, Texas, presented at 46th Annual SEG Meeting.

Bone, M. R., B. F. Giles, and E. R. Tegland, 1983, Analysis of seismic data using horizontal cross-sections: Geophysics, v. 48, p. 1172–1178.

Cordsen, A., M. Galbraith, and J. Peirce, 2000, Planning land 3-D seismic surveys: SEG Geophysical Developments, no. 9, 204 p.

French, W. S., 1974, Two-dimensional and three-dimensional migration of model-experiment reflection profiles: Geophysics, v. 39, p. 265–277.

Graebner, R. J., B. A. Hardage, and W. A. Schneider, 2001, 3-D seismic exploration: SEG Geophysics Reprint Series, no. 22, 857 p.

Lindsey, J. P., 1989, The Fresnel zone and its interpretive significance: The Leading Edge, v. 8, no. 10, p. 33–39.

Martins, C. C., C. A. da Costa, C. E Theodoro, L. R. Guardado, and V. F. Andrade, 1995, 3-D Seismic: A successful strategy in the Campos Basin: The Leading Edge, v. 14, p. 701–704.

Nestvold, E. O., 1992, 3-D seismic: Is the promise fulfilled?: The Leading Edge, v. 11, no. 6, p. 12–19.

Roberts, G. A., and M. J. Hughes, 1995, Workstation interpretation — a comparison of data stored at 8 and 16 bits: Poster paper and EAGE Annual Convention, Glasgow.

Schneider, W. A., 1998, 3-D seismic: A historical note: The Leading Edge, v. 17, p. 375–380.

Sheriff, R. E., 1985, Aspects of seismic resolution, *in* O. R. Berg and D. Woolverton, eds., Seismic stratigraphy II: An integrated approach to hydrocarbon exploration: AAPG Memoir 39, p. 1–10.

Sheriff, R. E., A. R. Brown, and R. M. Lansley, 2010, Fundamentals of reservoir geophysics, *in* D. H. Johnston, eds., Methods and applications in reservoir geophsics, Chapter 2: The supporting technologies: SEG Investigations in Geophysics Series No. 15, p. 101–122.

Tegland, E. R., 1977, 3-D seismic techniques boost field development: Oil and Gas Journal, v. 75, no. 37, p. 79–82.

Walton, G. G., 1972, Three-dimensional seismic method: Geophysics, v. 37, p. 417–430.